UPPSALA
UNIVERSITET

Digital Comprehensive Summaries of Uppsala Dissertations from the Faculty of Science and Technology 2143

Droplet Acoustofluidics for Biochemical Applications

ZHENHUA LIU

ACTA
UNIVERSITATIS
UPSALIENSIS
UPPSALA
2022

ISSN 1651-6214
ISBN 978-91-513-1488-4
URN urn:nbn:se:uu:diva-472081

Dissertation presented at Uppsala University to be publicly examined in Polhemsalen, Ångström Laboratory, Lägerhyddsvägen 1, 752 37 Uppsala, Uppsala, Monday, 30 May 2022 at 13:15 for the degree of Doctor of Philosophy. The examination will be conducted in English. Faculty examiner: Professor Nicole Pamme (Department of Materials and Environmental Chemistry, Stockholm University).

Abstract

Liu, Z. 2022. Droplet Acoustofluidics for Biochemical Applications. *Digital Comprehensive Summaries of Uppsala Dissertations from the Faculty of Science and Technology* 2143. 69 pp. Uppsala: Acta Universitatis Upsaliensis. ISBN 978-91-513-1488-4.

Droplet microfluidics is a promising platform for biochemical applications where compartmentalized droplets serve as individual vials. Droplets are formed by using two immiscible phases, the continuous phase and the dispersed phase, making up the droplets. Droplets are interesting because they can provide fast, parallel reactions with low reagent consumption. Microscale particles, such as cells, can be encapsulated in the droplets and chemical reagents can be added via a pico-injector. However, removal of droplet background signal is hard to achieved by conventional methods, especially if you do not want to risk losing the encapsulated cells. In this thesis, I present a droplet microfluidic system that can achieve this, via droplet-internal particle manipulation using acoustophoresis.

This droplet microfluidic system contains pico-injection and droplet split with acoustophoresis. The pico-injection is used to add fresh solution into the droplets and the droplet split with acoustophoresis is used to remove the droplet supernatant. With the combination of the pico-injector and the droplet split, the background signal of the droplets can be reduced and the cell medium in the droplets can be exchanged. This droplet microfluidic system can also be used to control timing of enzyme reactions by initiating the reaction by adding enzyme-coupled beads via the pico-injector and taking a sample from the droplets at specific time points via side channels. In this work, I have also investigated how the design of the droplet split could be optimized to obtain high particle recovery and enrichment. Finally, acoustic properties of a selection of oils that can used as the continuous phase were mapped to optimize the droplet system for acoustophoresis.

This thesis explores the biochemical applications performed by the droplet acoustofluidics, in-droplet time-controlled enzyme reaction and medium exchange for in-droplet cell culture. Furthermore, the droplet acoustofluidics has the potential to study the reaction kinetics by other enzymes and achieve long-term in-droplet cell culture.

Keywords: Droplet microfluidics, Acoustophoresis, Pico-injection, Droplet split, Biochemical reaction, In-droplet cell culture.

Zhenhua Liu, Department of Materials Science and Engineering, Microsystems Technology, Box 35, Uppsala University, SE-751 03 Uppsala, Sweden.

ISSN 1651-6214
ISBN 978-91-513-1488-4
URN urn:nbn:se:uu:diva-472081 (http://urn.kb.se/resolve?urn=urn:nbn:se:uu:diva-472081)

To my family

List of Papers

This thesis is based on the following papers, which will be referred by their roman numerals.

I. Liu, Z., Fornell, A., Barbe, L., Hjort, K., Tenje, M. (2019) On-chip background dilution in droplets with high particle recovery using acoustophoresis. *Biomicrofluidics*, 13(6):064123.

II. Fornell, A., Liu, Z., Tenje, M. (2020) Optimisation of the droplet split design for high acoustic particle enrichment in droplet microfluidics. *Microelectronic Engineering*, 226: 111303.

III. Liu, Z., Fornell, A., Tenje, M. (2021) A droplet acoustofluidic platform for time-controlled microbead-based reactions. *Biomicrofluidics*, 15 (3): 034103.

IV. Shi, Q., Liu, Z., Fornell, A., Werr, G., Barbe, L., Tenje, M. Mapping the acoustic properties of two-phase systems for use in droplet acoustofluidics. *Manuscript*.

V. Liu, Z., Agnihotri, S., Barbe, L., Fornell, A., Tenje, M. Long-term droplet cell culture enabled by droplet acoustofluidics. *Manuscript*.

Author's contribution

I. Most of designing, fabrication, experiment, analysis, and major part of writing.

II. Part of designing, experiment and writing, most of fabrication.

III. Most of designing, fabrication, experiment, analysis, and major part of writing.

IV. Part of designing, experiment and writing, most of fabrication.

V. Most of designing, fabrication and experiment, and part of analysis and writing.

Contents

Abbreviations

ALP	Alkaline phosphatase
BAW	Bulk acoustic wave
CAD	Computer aided design
ddPCR	digital droplet polymerase chain reaction
DEA	Diethanolamine
DEP	Dielectrophoresis
DI water	Deionized water
DMD	Digital micromirror devices
DNA	Deoxyribonucleic acid
DRIE	Deep reactive-ion etching
ELISA	Enzyme-linked immunosorbent assay
FDP	Fluorescein diphosphate
LFA	Lateral flow assays
IDT	Interdigitated transducers
IVD	In-vitro diagnostics
PBS	Phosphate buffered saline
PCR	Polymerase chain reaction
PDMS	Polydimethylsiloxane
PGPR	Polyglycerol polyricinoleate
PMMA	Polymethyl methacrylate
POCT	Point-of-care Testing
PZT	Lead zirconium titanate
SAW	Surface acoustic wave
UV	Ultraviolet
µTAS	Micro total analysis system

1. Introduction

1.1 Microfluidics

Microfluidics is a technology to manipulate fluids at a microscopic scale by miniaturizing the device. In the past century, many researchers from different fields have contributed to the development of microfluidics from theoretical understanding to practical applications. Physicists study the theory that enables predicting and controlling flow behaviours. Electrical and mechanical engineers develop functional systems on chip, such as mixers, micropumps and microvalves. Analytical chemists and biochemists explore the potential applications with better performance than conventional methods.[1]

The microfluidic system can be integrated with different analysis functions that should be performed in the lab, so it is commonly called micro total analysis system (μTAS) or Lab-on-a-Chip (Figure 1). Microfluidics is expected to take more important roles in in-vitro diagnostics (IVD). For example, lateral flow assays (LFA) has been widely used in point-of-care Testing (POCT), such as SARS-Cov-2 antigen tests. These tests fulfil the ASSURED criteria, affordable, sensitive, specific, user-friendly, rapid, equipment-free, and deliverable to end-users, which is addressed by the World Health Organization.[2] Apart from IVD and POCT, microfluidic technology has been widely used in other biomedical applications such as agriculture, food safety and single cell analysis.[3] With the rapid development of microfluidic technology, the global microfluidics market is projected to grow at a rate of 23.3% every year during the period from 2021 to 2026.[4, 5]

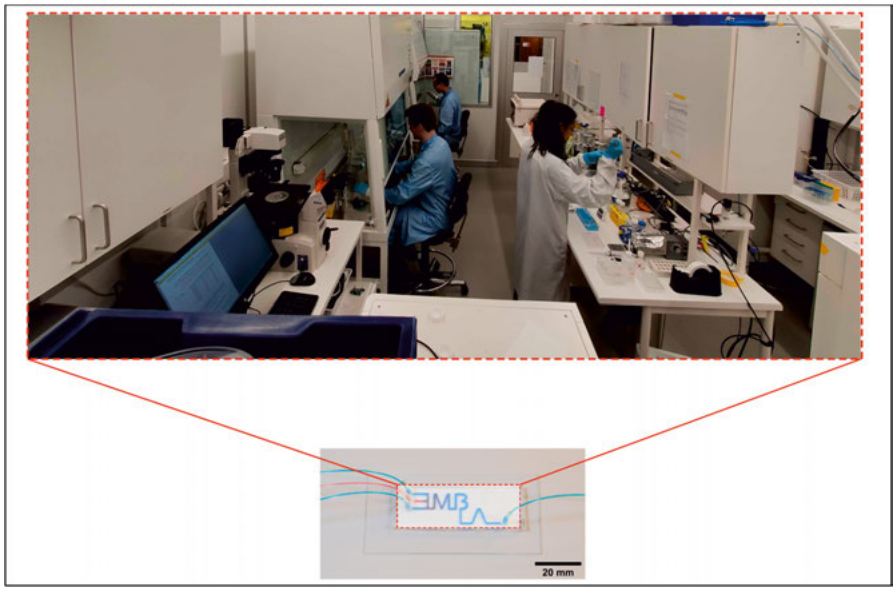

Figure 1 Concept of lab on a chip: the lab work can be performed on a microfluidic chip.

The typical microfluidic channel size ranges from a few micrometres to hundreds of micrometres. When the channel is comparable to the cells in size, precise manipulation of cells is possible by delicate design, such as cell sorting and separation.[6-8] Microfluidics can also create in vivo-like models for cell culture. These models can be controlled by the microfluidic platform and keep their metabolic function. It is expected to replace animal tests. For example, the microfluidic blood-brain barrier model has been demonstrated on drug permeability screening[9] and organ-on-a-chip mimics in-vivo microenvironment for cell growth and functional expression.[10] The cost is also reduced since less volume of fluid and less energy are required to operate a microfluidic device.

Microfluidic chips were firstly made by silicon and glass as there are sufficient methods to fabricate microstructure on silicon for microsystems technology devices. Now silicon and glass are still used to fabricate bulk acoustic chips[11] and high-pressure chips.[12] With the development of microfabrication technology, polymers take the dominating role in fabricating microfluidic chips.[13] The thermoset polymer, polydimethylsiloxane (PDMS) is the most used material for research on microfluidics and the thermoplastic polymer, polymethyl methacrylate (PMMA) is mostly used for commercially mass production.

1.2 Dimensionless numbers

Similar to microelectronics, microfluidics also benefits from scaling laws. The area-to-volume ratio of an object increases when shrinking the dimensions. The reactions in microfluidics are faster due to the high area-to-volume ratio. At the microscale, the surface forces (surface tension, viscosity) become more dominant than volume forces (gravity, inertia).[14] The dimensionless numbers are used to characterize the fluid dynamics. In this thesis, droplet-relative dimensionless numbers are discussed.

Reynolds number (*Re*) is the ratio between the inertial force and the viscous force in fluid.[15] When the droplet flows through the channel, *Re* of the continuous phase or the dispersed phase can be calculated in equation 1.1:

$$Re = \frac{\rho v D_h}{\eta} \tag{1.1a}$$

$$D_h = \frac{4A}{P_{wet}} \tag{1.1b}$$

where ρ is the density of the continuous phase or the dispersed phase, v is the flow velocity in channel, D_h is the hydraulic diameter in the channel, η is the viscosity of the continuous phase or the dispersed phase, A is the cross-section area of the channel, P_{wet} is the wetted perimeter at the cross section. At very low Re, the mixing is mainly dependent on diffusion rather than convection due to the high momentum diffusion and the low momentum convection in the fluid, that is called laminar flow.[14] In laminar flow, the fluids flow in layers and particles follow the streamlines (Figure 2). In microfluidics, the viscous force typically dominant over the inertial force, and that simplifies the prediction and manipulation of particle trajectories.

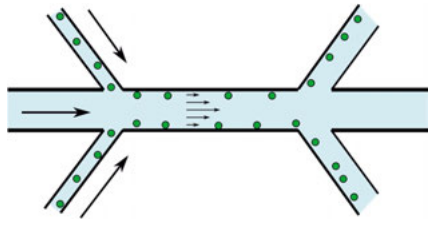

Figure 2 A microfluidic chip to show laminar flow.

Capillary number (*Ca*) presents the ratio between the inertial force and the interface force:[15]

$$Ca = \frac{\eta v}{\gamma} \tag{1.2}$$

where η is the liquid viscosity, v is the liquid flow velocity in channel, γ is the interfacial tension between the two immiscible phases. The capillary number is used to study two-phase flow, such as droplet flow and liquid filling in a pipe.

1.3 Droplet microfluidics

Droplet microfluidics is an important branch in microfluidics and it contains at least two immiscible phases, the dispersed phase and the continuous phase. Droplets can be formed when two immiscible fluids meet on a microfluidic chip and the volume of the droplets ranges from picolitres to nanolitres. The reaction rate in droplets can be improved as internal flow in the droplets boosts the mixing.[16] Thousands of droplets can be generated from several microlitres reagents in a short time and the sizes of droplets are highly monodisperse. Droplets can be used as microscopic containers for biochemical applications, such as intra-droplet biochemical reactions[17, 18] and cell-based assays.[19, 20] Digital microfluidics is another type of droplet microfluidics, where droplets are manipulated by an array of electrodes,[21] however digital microfluidics was not studied in this thesis.

To generate droplets in a microfluidic chip, it is common to use oil as the continuous phase and aqueous solution as the dispersed phase (Figure 3). The isolated droplet serves as an individual vial for reagents that can be dissolved or suspended in the aqueous solution. The reagents can be compartmentalized into thousands of droplets which is good for running parallel tests. If the reagent is not soluble in oil, the droplet is an ideal chamber to avoid cross-contamination. When the droplet flows in the channel, the internal circulating flow in the droplet enhances mixing and allows for fast reactions in the droplet.

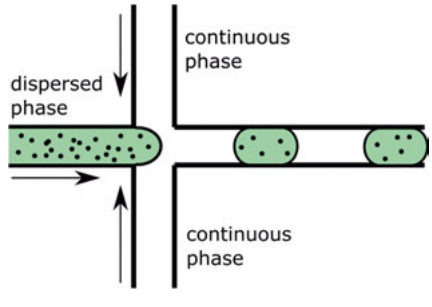

Figure 3 A microfluidic chip for particle encapsulation in droplets.

1.3.1 Biochemical applications

Droplet microfluidics can be used as a powerful analytical platform for biochemical applications.[22] Thousands of parallel reactions can be achieved in droplets with the requirement of much less reagents. The mixture ratio of components in droplets can be precisely controlled by the flow rates at each inlet. The detection of the product can be integrated on chip and that can increase the throughput for sample analysis.

Droplet microfluidics has been used to control enzyme reactions.[23] The enzyme reaction starts when the substrate meets the enzyme in the droplet after being pico-injected (Figure 4). The reaction time can be precisely recorded according to the position of the measurement points. Fluorescent products can easily be quantified by a fluorescence microscope or on-chip by two photon multiplier tube modules. This type of system can be used to study reaction kinetics with high throughput and low reagent consumption.[17] For a library of droplets containing mutated cells that can secret enzyme, this system can be used to screen the specific variants for example the cells with higher enzyme production .[24]

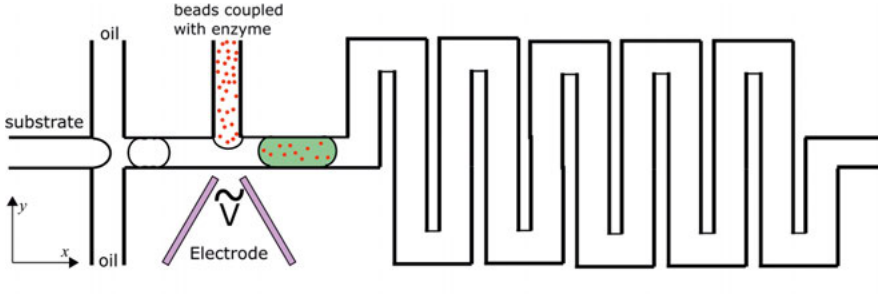

Figure 4 A microfluidic chip to study enzyme reactions in droplets.

The Polymerase chain reaction (PCR) is an important tool to amplify deoxyribonucleic acid (DNA) for genetic research.[25] Droplet digital PCR (ddPCR) has shown high sensitivity and accuracy in cancer research. As the DNA sample is compartmentalized into thousands of droplets with high uniformity, thousands of parallel PCR reactions can take place in each droplet.[26] The ddPCR has been used in medical diagnosis, such as SARS-Cov-2 testing.[27, 28] The enzyme-linked immunosorbent assay (ELISA) is widely used to detect biomarkers, such as proteins. Droplet digital ELISA has shown higher sensitivity than conventional ELISA by improving the sampling efficiency.[29]

Nanoparticles exhibit special optoelectronic properties and chemical activities in catalysis, sensing and photonics.[30] Droplet microfluidics provides a flexible platform for nanoparticle synthesis. For example, metal nanoparticle shape

can be changed by varying the flow rates of each reagent and reaction temperature.[31] The size of ceramic nanoparticles can be adjusted by changing the reaction time and the reagent concentration.[32]

1.3.2 Cell-based applications

Droplet microfluidics has been widely used for cell-based applications as it can create a controlled microenvironment for cell growth and it is able to precisely manipulate the fluids at the cell scale. All products secreted by the cells are confined inside the droplet and the undiluted products are easy to detect. Cross-talk and cross-contamination can be eliminated by ensuring that the droplets are stable and do not interact with each other.

The heterogenetic information of each cell is hidden when a group of cells is analysed.[33] Single-cell analysis such as fluorescence-based flow cytometry is used to reveal the information at the single-cell level. With compartmentalization of cells into droplets, it is possible to parallelly monitor the life span and the dynamic growth of each individual cell. High-throughput screening of cells for specific applications, such as enzyme screening,[24] antibody screening[34] and dose-response screening[35] can be achieved.

Droplets can create a scaffold structure for cell culture to protect cells from shear force (Figure 5).[36] Hydrogels are widely used as a 3D scaffold for cell culture as the cross-linked hydrogel is solid and biocompatible. The hydrogel droplet can create a microenvironment for cancer spheroid growth and anticancer drug testing.[10]

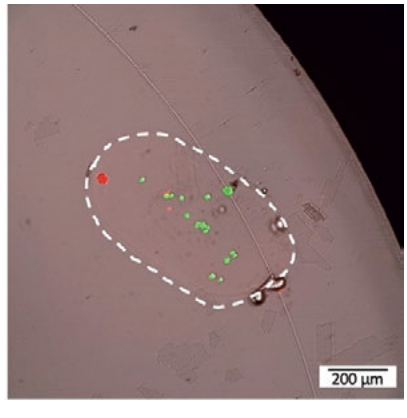

Figure 5 The cells are encapsulated in the hydrogel droplets. Reprinted with permission from ref. 36. Copyright 2021 Springer Nature.

1.4 Scope of thesis

Droplet-internal particle manipulation is challenging as the droplets are too small to be manipulated by conventional methods. For example, solution exchange which is required for washing cells can be performed by centrifuging cell medium to isolate cells and adding fresh cell medium. But this method is hard to perform in droplets as droplets will coalescence after centrifugation. The aim of this thesis is to develop a droplet microfluidic system to manipulate droplets for biochemical applications. Particles in droplets can be focused by acoustophoresis (Figure 6a) and droplets can be injected with other fluids by the pico-injection (Figure 6b). By this way, the individual droplet can be added and separated fluid in a chip that makes it possible for solution exchange without losing the encapsulated particles.

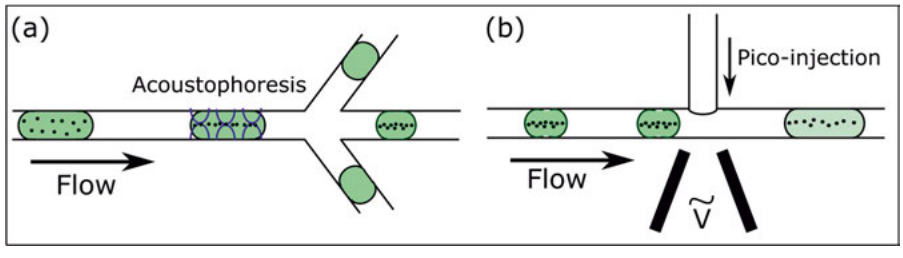

Figure 6 (a) Droplet split with high particle recovery by acoustophoresis. (b) The volume of the droplet gets increased by pico-injection, so the concentration of the background is diluted.

Paper I presents a microfluidic system for on-chip background dilution of droplets with high particle recovery by integrating acoustophoresis and pico-injection on chip. Paper II optimized the droplet split design for higher particle enrichment. Paper III presents a droplet microfluidic platform for time-controlled enzymatic reaction. Paper IV is focused on the acoustic properties of a selection of oils that can be used in droplet microfluidics. In Paper V, a droplet microfluidic chip is developed to exchange the cell medium on chip for extending in-droplet cell culture.

2. Droplet dynamics

2.1 Droplet generation

In microfluidics, droplets are generated by pinching-off dispersed phase in the continuous phase in a channel. The droplets can be actively generated by external field, such as mechanical pressure field,[37] electric field,[38] magnetic field[39] and acoustic field.[40, 41] Active droplet generation has higher flexibility in controlling droplet size and droplet rate, and it enables on-demand droplet generation. Moreover, it takes shorter time to stabilize droplet generation.[42] In contrary to active methods, passive droplet generation relies only on channel geometry and flow rates to control the generation rate and droplet size, without the need of other external fields. The flows are usually driven by syringe pumps, pressure pumps, or gravity. For water-in-oil droplet generation, the channel should be hydrophobic to make sure there is a thin film of the continuous phase between the droplet and the channel wall.

2.1.1 Geometry

There are many different methods to generate droplets on chip, but the geometries of the channels used for droplet generation are similar. There are three types of channel geometry for droplet generation: cross-flow design, flow-focusing design and co-flow design.

In the cross-flow design (Figure 7a), the dispersed phase meets the continuous phase at the 'T junction' and breaks into droplets due to the shear force and the interfacial tension.[42] The cross-flow design can generate highly monodisperse droplets with simple design. However, the minimal droplet size is limited by the channel dimension. There is a risk that the droplets could adhere to the channel if the channel is not hydrophobic enough as the breakup occurs at the wall of the 'T junction'.[22]

In the flow-focusing design (Figure 7b), the dispersed phase is squeezed and elongated at the orifice of the junction, and that makes it possible to generate small droplets at high flow rates.[42] This design is more complex than the cross-flow design and it requires more space on the chip for extra channels and inlets.

In the co-flow design (Figure 7c), the dispersed phase flows in an inner channel that is coaxially inserted by an outer channel filled with the continuous phase.[42] The size of droplets is larger than the dimension of the dispersed phase channel at low flow rates. Polydisperse droplets could occur at high flow rates.

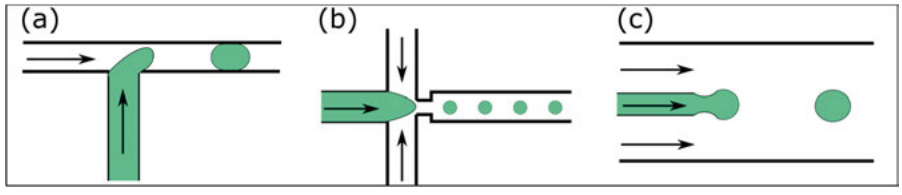

Figure 7 Channel geometries for droplet generation. (a) cross-flow design, (b) flow-focusing design, (c) co-flow design. The white fluid represents the continuous phase and the green fluid represents the dispersed phase.

2.1.2 Droplet breakup

There are three droplet breakup models which can be characterized by the capillary number (Ca).[30] When the continuous phase flows at a low Ca where the viscous force is negligible, the dispersed phase is squeezed by the channel to form a 'plug' at the junction. That plug induces a growth of pressure gradient in the continuous phase and it will be pinched-off into a droplet when the pressure gradient is large enough (Figure 8a). When Ca of the continuous phase increases, the viscous shear force is large enough to pinch-off the droplets before the plug is formed (Figure 8b). When Ca of the continuous phase increases further, the viscous force is dominating over the interfacial tension. The continuous phase is extended in the continuous phase and breaks up into droplets after the jet (Figure 8c).

Figure 8 Droplet breakup modes: (a) squeezing, (b) dripping, (c) jetting. Scale bar:200 μm.

2.1.3 Particle encapsulation

When particles are encapsulated in droplets, the number of encapsulated particles in each droplet follows the Poisson distribution. The probability (P) of droplets encapsulating k particles can be determined by equation 2.1:

$$P(k,\lambda) = \frac{\lambda^k e^{-\lambda}}{k!} \tag{2.1}$$

where k is the number of particles in a droplet and λ is the average number of particles per unit droplet volume. When λ=1, P(0,1)=37%, P(1,1)=37%, P(2,1)=18% which means that among the generated droplets, 37% of the droplets will have only one particle encapsulated, 37% of the droplets will be empty, 18% of the droplets will contain two particles and 8% of the droplets will contain more than two particles. For single-cell encapsulation, the concentration of particle solution should be low enough to make sure most of the generated droplets contain no more than one particle. However, it will generate a large number of empty droplets, that could cause waste of reagent and increasing the sampling size.

2.2 Oil and surfactant

In droplet microfluidics, water-in-oil droplets are widely used for biochemical applications. Silicone oils, hydrocarbon oils and fluorinated oils are the most used oils as continuous phase in droplet microfluidics. The light-viscosity silicone oils swell PDMS and that limits the usage in PDMS chip.[43] The hydrocarbon oils (mineral oil, linseed oil, olive oil and sunflower oil) could dissolve some organic reagents.[44] Fluorinated oils (HFE-7500 and FC-40) show good match for droplet microfluidics, due to the low viscosity, high gas permeability, low solubility for most solvents.[45] Hydrocarbon oils show better matched acoustic properties with water and that is good for acoustic wave propagation through droplets.[46]

A surfactant is a type of amphiphilic reagent that can be used to prevent droplet coalescence. The typical surfactant molecule contains a hydrophilic end and a hydrophobic end and it will diffuse to the water/oil interface. When droplets contact each other, the existence of surfactant and the Marangoni effect induced by the surfactant gradient prevent the drainage of the oil film between droplets.[45]

Table 1 Viscosity, speed of sound, density and acoustic impedance of oils.[47]

		Viscosity (mPa·S)	Speed of sound (m/s)	Density (kg/m^3)	Acoustic impedance (Pa·s/m)
Water		0.9	1,497	997	1,492,509
Silicone oil (50 cSt)		50	1,046	960	1,004,160
Hydrocarbon oil	Light mineral oil	16.4	1,428	845	1,206,660
	Heavy mineral oil	67.7	1,488	859	1,278,192
	Linseed oil	29	1,462	925	1,352,350
	Olive oil	40	1,459	910	1,327,690
	Sunflower oil	48.8	1,458	915	1,334,070
Fluorinated oil	HFE-7500	0.8	710	1,618	1,148,780
	FC-40	4.1	687	1,866	1,281,942

For biochemical applications, the emulsion including oil and surfactant should be biocompatible. For example, a surfactant which can absorb or deactivate proteins cannot be used in biochemical application (Figure 9).[48] The surfactant may cause molecular exchange between the droplets or molecular leakage from the droplet. In this thesis, light mineral oil is used as the continuous phase and the surfactants used are span 80, EM 90 and polyglycerol polyricinoleate (PGPR). Span 80 and EM 90 have been used in droplet microfluidics for biochemical applications[45] and PGPR is an emulsifier for water-in-oil emulsification in food industry.

As an alternative to standard surfactants, modified-amphiphilic silica nanoparticles can work as surfactants in water-in-oil droplets.[49]

Surfactants are a critical component in the continuous phase for stabilizing the droplets. In Paper I and Paper II, span 80 was added in mineral oil to prevent droplet coalescence when the adjacent droplets contacted each other in the channels. In Paper III and Paper V, PGPR was added in mineral oil to prevent

droplet coalescence when droplets were collected in a PDMS chip for off-line analysis.

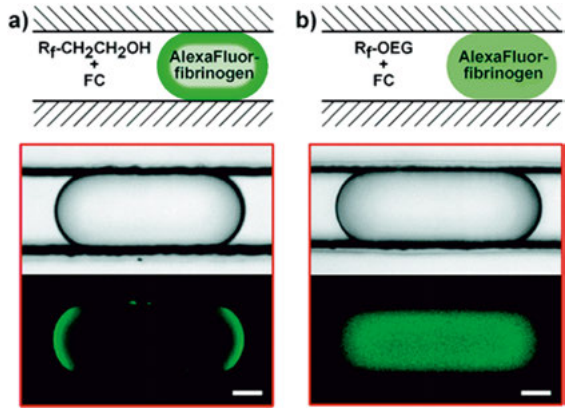

Figure 9 (a) Increased fluorescence at the droplet interface indicates absorption of protein at the interface. (b) Uniform fluorescence across the droplet indicates few absorptions of protein at the interface. Reprinted with permission from ref. 48. Copyright 2005 American Chemical Society.

2.3 Droplet manipulation

2.3.1 Mixing

In microfluidics, since the Reynolds number is much smaller than the critical value of laminar flow, diffusion dominates over convection so that longer times are required to obtain good mixing. However, good mixing is essential for on-chip reaction. For single phase flow, the channel geometry can be adjusted to obtain passive mixing or external force for active mixing can be used.[50] But in droplets, the droplet-internal circulation flow makes passive mixing fast. When the droplet flows through the serpentine channel, the droplet gets stretched and folded and that process enhances mixing inside droplets (Figure 10).[51]

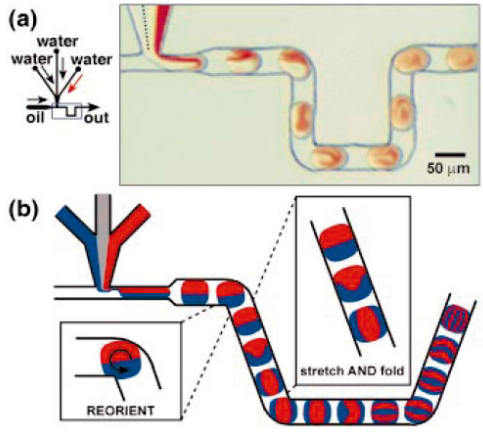

Figure 10 (a) Images of droplet mixing in serpentine channel. (b) Droplet circulation flow in serpentine channel. Reprinted with permission from ref. 51. Copyright 2003 American Institute of Physics.

2.3.2 Coalescence

Droplet coalescence occurs to minimize the total interfacial energy of the system. Surfactants are added in droplet microfluidics to prevent unwanted droplet coalescence, as discussed above. However, sometimes reagents need to be added to the existing droplets for in-droplet enzymatic reactions[17] and controlled reactions,[52] thus selective and controllable methods of droplet coalescence are required. Common methods for controlled droplet coalescence include merging of a pair of droplets and injection from the side channel (Figure 11). A pair of droplets can be merged by collision where design features make the rear droplet "catch up" with the front droplet trapped in the pillar array[53] or at the expanding channel,[54] and then two droplets merge due to the droplet collision. Droplet pairs can also be merged by electric field[55], optical heating[56] and acoustics.[57] The droplet can be injected with fluid from the side channel by electric field[58] or a capillary tubing,[52] and that technique is called pico-injection. These methods show their ability of selective and controllable injection.

In this thesis, pico-injection is used to add other fluids into the droplets. The same design as in Figure 11b is used, as it is simple to design and easy to fabricate. A pair of electrodes are integrated opposite to the side channel. When an alternating current applies on the electrodes, the droplets get pico-injected by electrocoalescence.

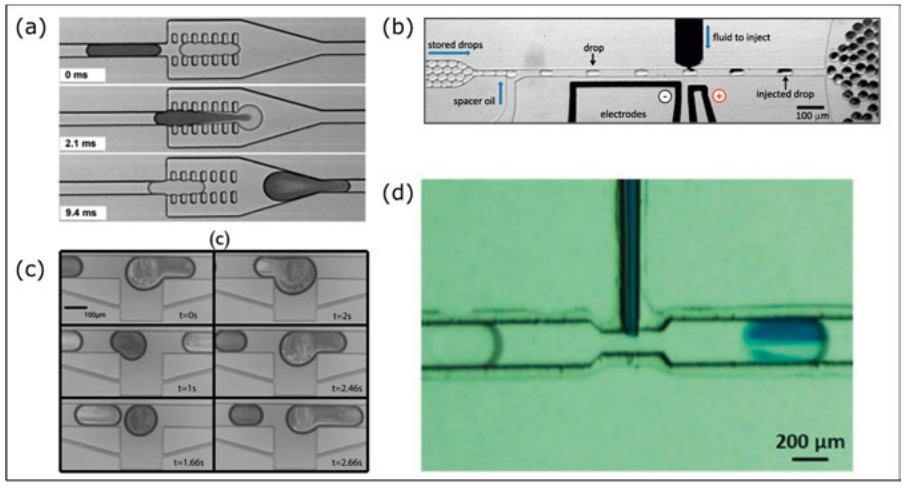

Figure 11 (a) Passive droplet coalescence by droplet collision. Reprinted with permission from ref. 53. Copyright 2008 Royal Society of Chemistry. (b) Active droplet coalescence by pico-injection. Reprinted with permission from ref. 58. Copyright 2010 National Academy of Sciences. (c) Active droplet coalescence by acoustics. Reprinted with permission from ref. 57. Copyright 2014 Royal Society of Chemistry. (d) Passive droplet coalescence by capillary tubing. Reprinted with permission from ref. 52. Copyright 2017 Wiley.

2.3.3 Split

A droplet can be divided into several daughter droplets for particle enrichment[59, 60] and high-throughput droplet generation.[61] The droplet split can be categorized into passive methods and active methods (Figure 12). When a plug droplet flows through a channel with more than one outlet, the plug droplet will be split into each outlet and the split ratio is dependent on the flow rates of each outlet. For active methods, an external force is needed to split the droplets, such as acoustic waves,[62] an electric field,[63] or a pressure valve.[64]

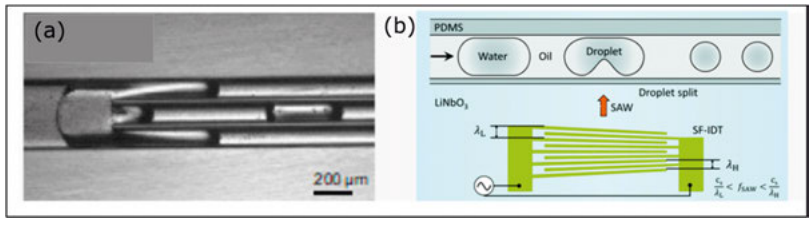

Figure 12 (a) Passive droplet split by a trifurcation channel. Reprinted with permission from ref. 59. Copyright 2020 Elsevier. (b) Active droplet split by acoustic waves. Reprinted with permission from ref. 62. Copyright 2016 Royal Society of Chemistry.

2.3.4 Particle manipulation

When particles are encapsulated inside droplets, the number of particles in each droplet will be determined by the Poisson distribution, as discussed above. Particle manipulation is a crucial step for bead-based assays. Microfluidics has shown the powerful ability to manipulate particles in single phase flow by both active manipulation and passive manipulation.[6] However, for droplet microfluidics, particle manipulation methods need more consideration to overcome the droplet-internal circulation flow and the water/oil interface. Only a few passive methods can be used for in-droplet particle manipulation whereas active methods such as magnetophoresis, dielectrophoresis and acoustophoresis are more suitable for in-droplet particle manipulation (Figure 13).

(1) Hydrodynamics

For single phase microfluidics, hydrodynamics is widely used for particle manipulation, such as inertial focusing[65] and pinched flow fractionation.[66] In droplet microfluidics, hydrodynamics can only work for particle manipulation in a limited situation. The particles should have large dimension or large density to obtain high sedimentation velocity for accumulation. For cells and other particles with low density, long droplets and slow flow are required for successful particle accumulation.[67]

(2) Magnetophoresis

A gradient magnetic field can be used to manipulate magnetic particles or magnetic fluids. Magnetophoresis requires a non-uniform magnetic field induced by an external magnetic source, usually a permanent magnet[68] or an electromagnet.[69] Magnetic particles will be arranged as chains following along the magnetic field lines because of the inter-particle interactions by the magnetic moments[70] However, magnetophoresis requires labelling of the bio-samples with magnetic particles. Magnetic particles with the affinity of different ligands are commercially available and that makes magnetophoresis work for cell separation,[71] protein purification and DNA isolation.[72]

(3) Dielectrophoresis

Dielectrophoresis (DEP) is a label-free method for particle manipulation using an external electric field. Electric dipoles are formed on the polarized particles when exposed to a non-uniform electric field and the DEP force is exerted on these dipoles. Particles can be manipulated by the DEP force depending on their dielectric properties and surrounding solutions. As cells and cell medium (mostly water) have different dielectric properties, DEP can be used in cell-based applications.[60]

(4) Acoustophoresis

Acoustophoresis is another label-free method for particle manipulation, and it has been demonstrated to separate cells with high throughput and good biocompatibility.[73, 74] In droplet microfluidics, traveling surface acoustic waves can push particles to the opposite side in the droplet[75] and standing bulk acoustic waves can focus particles in the centre or side of the droplet depending on the acoustic contrast factor of the particle[76] and the acoustic harmonic mode.[77]

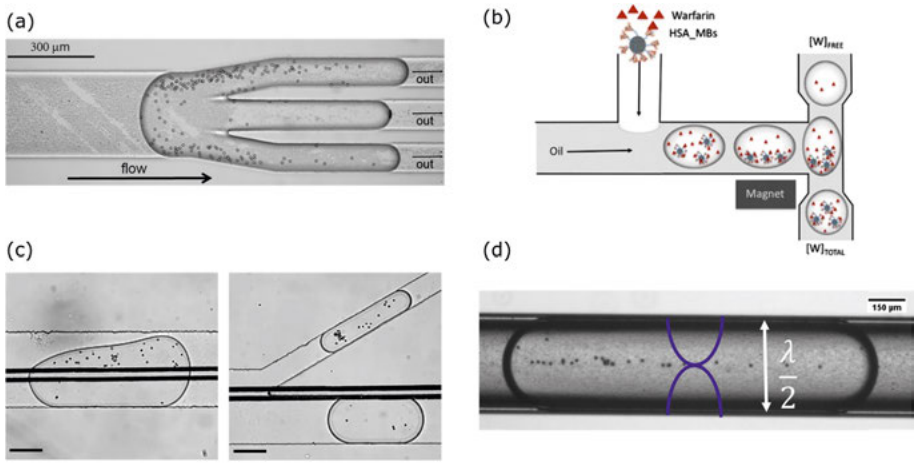

Figure 13 In-droplet particle manipulation by (a) hydrodynamics (Reprinted with permission from ref. 67. Copyright 2015 Royal Society of Chemistry), (b) magnetophoresis (Reprinted with permission from ref. 68. Copyright 2010 Springer-Verlag), (c) dielectrophoresis, (d) acoustophoresis (Reprinted with permission from ref. 60. Copyright 2017 Elsevier).

3. Acoustofluidics

Acoustofluidics is the term used for the technologies that applies acoustic waves in microfluidics, such as acoustic focusing, acoustic streaming and acoustic trapping. Acoustofluidics provides a label-free and biocompatible method to manipulate microscale objects and fluids in biochemical applications as acoustic manipulation is a contactless and gentle force.

3.1 Acoustic focusing

Particles or cells can be focused by standing acoustic waves (Figure 14a). By this way, cell focusing can be used to improve single-cell printing efficiency,[78] and acoustic focusing can achieve thousand-fold enrichment of cells and shows little influence on the viability.[79]

Droplet encapsulated particles can also be enriched by acoustic focusing (Figure 14b).[59] The droplet split combined with acoustic focusing makes it possible to enrich particles in a droplet by reducing the droplet volume.

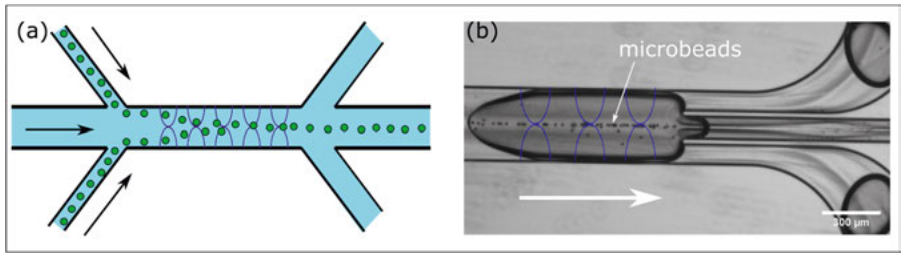

Figure 14 (a) Particles migrate from side to centre by acoustic focusing. (b) Particles are focused in the droplet.

3.2 Acoustic waves

3.2.1 Generation of acoustic waves

(1) Piezoelectricity

In acoustofluidics, the acoustic waves are commonly generated by the piezoelectric effect, which converts electrical signals to mechanical vibrations and *vice versa* (Figure 15). Piezoelectric materials that can exhibit piezoelectric effect, includes single crystals, polycrystalline ceramics and polymers. The polycrystalline lead zirconium titanate (PZT) is mainly used to generate bulk acoustic waves (BAWs), and the single crystal lithium niobate ($LiNbO_3$) is mainly used to generate surface acoustic waves (SAWs).

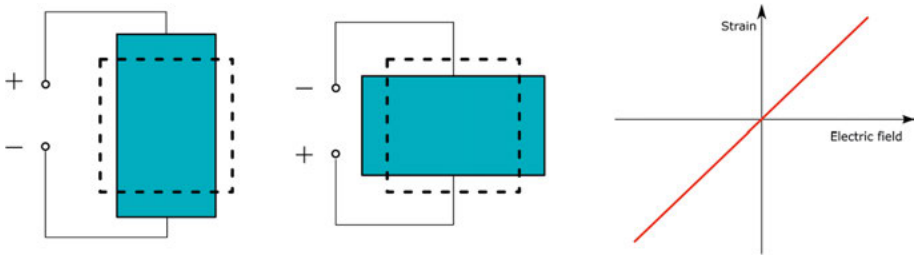

Figure 15 Schematic of the piezoelectric effect. The strain of the piezoelectric material is proportional to the applied electric field.

In this thesis, PZT elements were used to generate the acoustic waves. When a sinusoidal electric field is applied to the PZT element, acoustic waves with the same frequency will be generated by the vibrating of the PZT element. The primary frequency of PZT is determined by the composition of the ceramic material and the shape and volume of the element. In Paper I to Paper IV, PZT elements with the primary frequency of 2 MHz were used and in Paper V, PZT elements with the primary frequency of 5 MHz were used.

(2) BAW

In acoustophoresis, BAW is used to generate standing waves at the resonance mode for acoustophoresis. A typical BAW resonance chip contains a matching layer with channels, a piezoelectric transducer attached on the matching layer by a coupling layer, and a reflector layer (Figure 16). The characteristic acoustic impedance (Z) of the material is determined by Equation 3.1:

$$Z = \rho c \tag{3.1}$$

where ρ is the density and c is the speed of sound in the material.

When the acoustic waves travel through different materials, acoustic reflection and transmission will happen at the interface. For normal incidence of the acoustic waves, the pressure reflection coefficient (R_p) is given by

$$R_P = \frac{Z_2 - Z_1}{Z_2 + Z_1} \tag{3.2}$$

where Z_1 is the characteristic acoustic impedance of the first material and Z_2 is the characteristic acoustic impedance of the second material. To avoid acoustic losses due to reflection in standing BAW resonance, the characteristic acoustic impedance of the matching layer should be significantly larger than that of the fluid in the channel but smaller than that of the piezoelectric transducer (Figure 16).

When a half-wavelength standing BAW is generated in a channel, the pressure (p) is a function of the position (z) and time (t):

$$p(z,t) = p_a cos(kz) sin(\omega t) \tag{3.3}$$

where p_a is the amplitude of the pressure field, k is the wave number ($k=2\pi/\lambda$), ω is the angular frequency ($\omega = 2\pi f$).

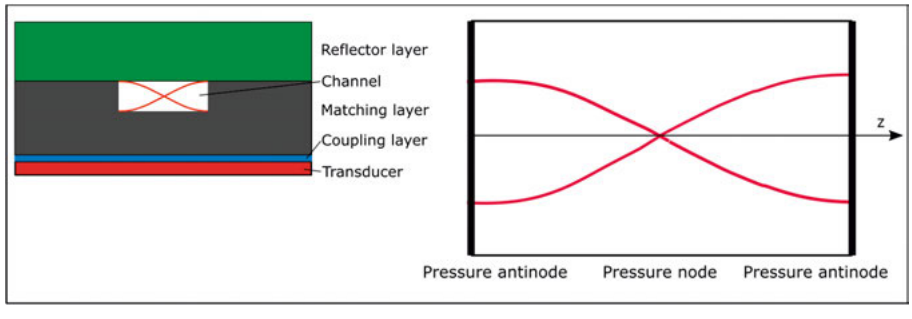

Figure 16 Schematic of a BAW resonance chip.

When the acoustic waves travel from the water in the channel to the silicon wall, R_P= (19790190-1492509)/(19790190+1492509) = 86%. When the acoustic waves travel from the water in the channel to a PDMS wall, acoustic resonance cannot be formed due to the poor acoustic reflective abilities at the water/PDMS interface and the high attenuation of acoustic waves in PDMS.[11] Silicon is a suitable material for BAW resonance due to the high acoustic impedance. However, acoustic reflection in e.g. PMMA channels is very low, which means such system requires higher power to actuate the acoustic resonance. As high power applied on piezoelectric transducer will cause increasing temperature due to Joule heating, PMMA and other polymer chips are not commonly used in BAW resonance systems. In this thesis, another advantage

of silicon is that the channels are formed by dry etching, which makes it possible to fabricate vertically straight channel walls for BAW resonance.

Table 2 Density, speed of sound and characteristic acoustic impedance for some materials.[80, 81]

	Density (kg/m^3)	**Speed of sound (m/s)**	**Characteristic acoustic impedance (Pa·s/m)**
Silicon	2,331	8,490	19,790,190
Borofloat® 33	2,200	5,560	12,232,000
Aluminium	2,700	6,420	17,334,000
PDMS	965	1,076	1,038,340
PMMA	1,150	2,590	2,978,500
Deionized water	997	1,497	1,492,509
Light Mineral oil	845	1,388	1,172,860
PZT	7,700	4,000	30,800,000
Air	1	343	343

(3) SAW

SAWs are generated by interdigitated transducers (IDTs) and the waves travel along the surface of piezoelectric materials, such as $LiNbO_3$. Compared to the BAW, IDTs can generate SAWs with higher frequency, from megahertz to gigahertz. SAW can work with PDMS chips, which simplifies the chip fabrication. SAWs can manipulate particles in both travelling SAW mode[82] and standing SAW mode.[83] The travelling SAW generated by a single IDT can push particles to the opposite wall. The standing SAW can be generated by a pair of IDTs and it can work to focus particles at nodes or antinodes similar to standing BAW.

3.2.2 Particle manipulation

(1) Primary acoustic radiation force

In the half-wavelength standing acoustic waves, the particles move to the nodes or antinodes by the primary acoustic radiation force:[84]

$$F^{rad} = 4\pi\Phi(\tilde{\kappa},\tilde{\rho})ka^3E_{ac}sin(2kz) \quad (3.4\ a)$$

$$\Phi(\tilde{\kappa},\tilde{\rho}) = \frac{1}{3}\left[\frac{5\tilde{\rho}-2}{2\tilde{\rho}+1} - \tilde{\kappa}\right] \quad (3.4\ b)$$

$$\tilde{\rho} = \frac{\rho_{particle}}{\rho_{fluid}} \quad (3.4\ c)$$

$$\tilde{\kappa} = \frac{\kappa_{particle}}{\kappa_{fluid}} \quad (3.4\ d)$$

where Φ is the acoustic contrast factor of the particle, ρ is the density, κ is the compressibility, k is the wave number ($k=2\pi/\lambda$), a is the radius of the particle, and E_{ac} is the acoustic energy density, z is the position cross the channel.

In a half wavelength acoustic resonator, for particles with a positive acoustic contrast factor, the primary acoustic radiation force moves the particles towards the pressure nodes. For particles with a negative acoustic contrast factor, the primary acoustic radiation force will move them towards the pressure anti-nodes (Figure 17). The primary acoustic radiation force is derived based on the assumption of the small particles in the inviscid fluid at the no-slip boundary condition.[84] For this to hold true, the particle radius should be larger than the boundary layer and smaller than the acoustic wavelength.[84] For example, the acoustic streaming will significantly affect behaviour of the polystyrene particles if the dimension of the particle is less than 1 μm.[85]

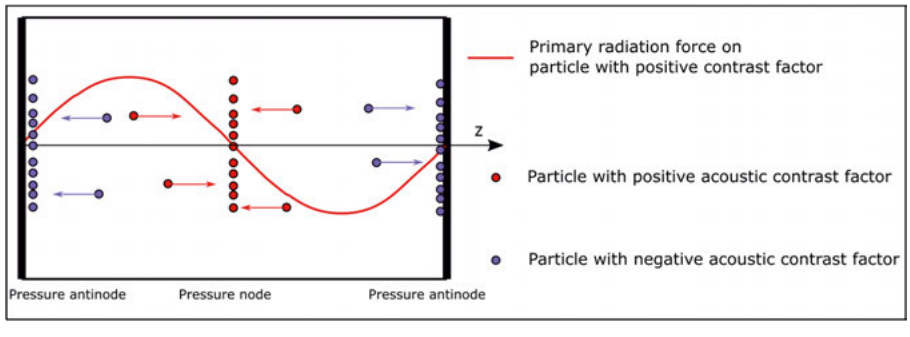

Figure 17 The primary radiation force distribution along the channel width.

(2) In-droplet particle manipulation

In this PhD thesis, standing BAWs are used to focus particles inside droplets. When using hydrocarbon oils, improved particle focusing ability inside droplet by BAW resonance has been observed, compared to using fluorinated oils.[46] In a long droplet (i.e. a 'plug'), particles can be focused in the middle

of the droplet and diverged at the rear end of the droplet (Figure 18a). In a short droplet, it is more difficult to get the particles focused by the same standing BAWs (Figure 18b). The standing BAWs work well for particle focusing in droplets using light mineral oil (Figure 18c).

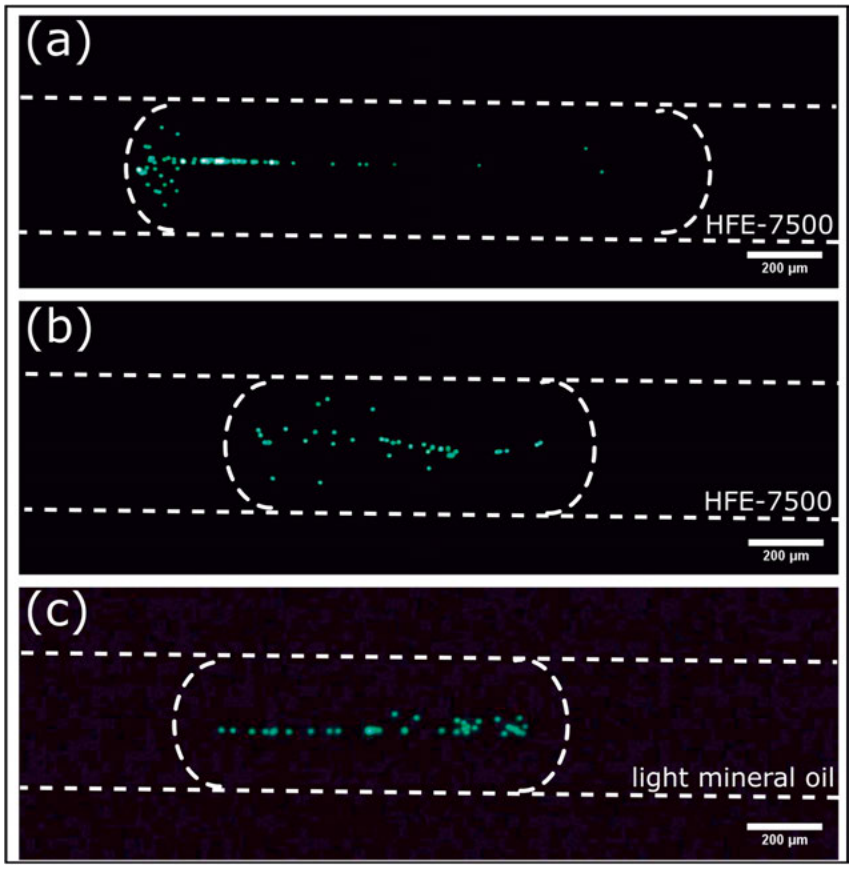

Figure 18 Particle (10µm diameter) focusing by standing BAWs in droplet surrounded by (a,b) HFE-7500 and (c) light mineral oil.

3.2.3 Applications of acoustophoresis

As discussed above, acoustophoresis is a technology that can be used to manipulate particles by acoustic waves in microfluidic systems. This section will highlight a few examples where the technology can be used.

(1) Washing

Two fluids in a microfluidic channel will flow in parallel without mixing due to the principles of laminar flow. Cells can be focused at the pressure node, located at the centre of the channel if a half wavelength standing acoustic wave

is set-up, so that cells can be washed when they migrate across the medium interface (Figure 19a).[86, 87]

Droplets containing cells can be washed in a similar way (Figure 19b). The old medium can be removed by droplet split while the cells can be retained by acoustic focusing. By injecting fresh medium into the droplets, the background signal can be reduced.[88]

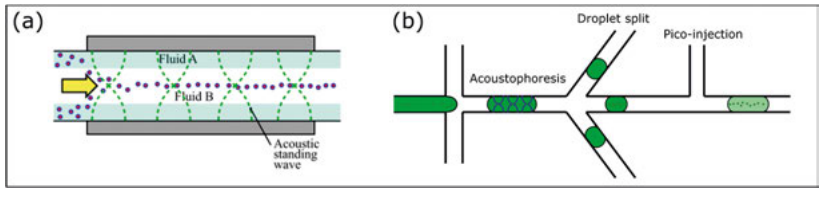

Figure 19 (a) Particle washing by acoustic focusing in parallel co-flow. Reprinted with permission from ref. 87. Copyright 2012 Royal Society of Chemistry. (b) In-droplet particle washing including acoustophoresis, droplet split and pico-injection.

(2) Separation

Acoustophoresis can also separate particles based on size,[89] density[90] and acoustic contrast factor.[91] To be efficient, it requires pre-alignment of the particles since the separation is based on the displacement from the pre-aligned position to the focusing position. It has been demonstrated to separate circulating tumour cells from white blood cells with high viability (Figure 20a).[92] Another approach based on the acoustic contrast factor is to bind the white blood cells to elastomeric particles with a negative acoustic contrast so that the cancer cells can be separated from the white blood cells (positive acoustic contrast factor) as the two different cell types will migrate to different positions in the acoustic pressure field (Figure 20b).[91]

Acoustophoresis has also been demonstrated to separate PDMS particles and polystyrene particles in droplets as PDMS particles have a negative acoustic contrast factor and polystyrene particles have a positive acoustic contrast factor. (Figure 20c).[76]

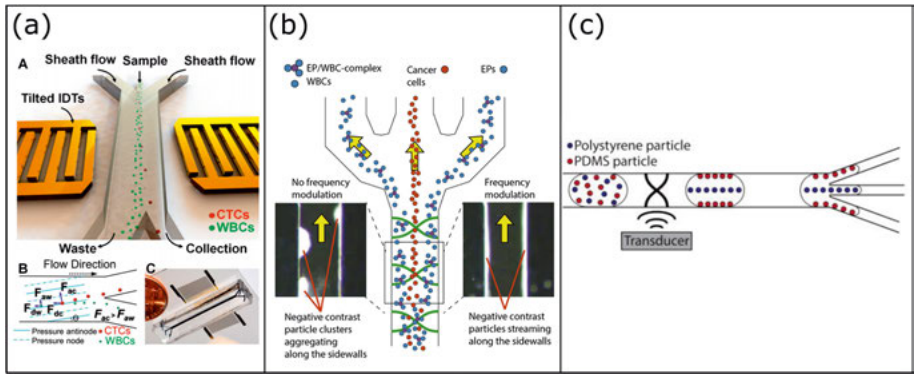

Figure 20 Particle separation by acoustophoresis based on (a) particle size (Reprinted with permission from ref. 92. Copyright 2015 National Academy of Sciences.) and (b) the acoustic contrast factor of the particles (Reprinted with permission from ref. 91. Copyright 2018 Elsevier). (c) Particles can be separated in droplet by acoustophoresis based on the acoustic contrast factor of the particles. Reprinted with permission from ref. 76. Copyright 2018 American Institute of Physics.

(3) Sorting

Acoustophoresis can also be used for sorting of fluorescently labelled particles when combined with fluorescence-activated cell sorting.[93] For single-cell encapsulation in droplets, a large amount of empty droplets will be generated according to the Poisson distribution. To remove the empty droplets, droplets containing fluorescently labelled cells can be detected and sorted out with high purity (Figure 21).[94]

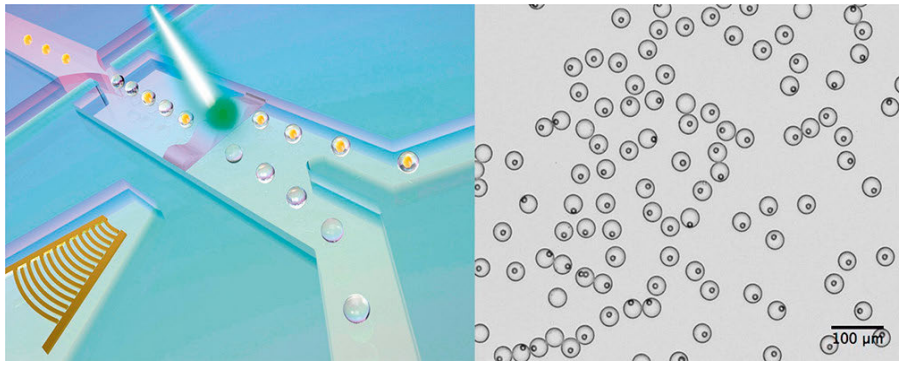

Figure 21 Droplets containing fluorescently labelled cells can be sorted by acoustics combined with fluorescence detection. Reprinted with permission from ref. 94. Copyright 2019 American Chemical Society.

4. Methods

4.1 Chip fabrication

Microfluidic devices are often fabricated in polymers but glass and silicon can also be used. To realise such devices, advanced cleanroom processing is often required as even the small dusts or fibres in the air could ruin the microstructures during fabrication. When preparing devices in glass and silicon, subtractive fabrication methods are used, where the microchannels are fabricated by removing part of the bulk material. This is often achieved via etching, where a photoresist is used as an etch mask. For the microfluidic chips with large channels, there are some photolithography-free methods that do not require use of a cleanroom. For example, lasers can be used to etch on substrate, such as silicon,[95] glass[96] and PMMA[97] directly from the digital computer aided design (CAD). With the development of laser technology, laser ablation has been widely used in microfluidic chip fabrication as it is fast, cheap and easy to use. However, the rough surface made by laser ablation cannot meet the requirement of smooth channels. 3D printing is another photolithography-free technology for direct microfabrication from digital CAD.[98] The unique advantage is the ability to fabricate arbitrary 3D structures with high resolution. But the lack of optical transparency of 3D printable materials is the main limitation for on-chip observation and detection. Injection molding and hot embossing of PMMA or polycarbonates are the most used methods for mass production.

This chapter describes the fabrication steps involved when preparing microfluidic devices in a cleanroom. The steps can either be used to define the channel in silicon, or to prepare a master mould in silicon (or SU-8) that can be used to fabricate microfluidic chips in polymers by soft lithography.

4.1.1. Materials

Before PDMS was applied in microfluidics, silicon was the standard material used in microfabrication of semiconductor devices. Now silicon is still an important material for some special applications. For example, silicon has high tolerance of solvent and silicon chips can be used in high pressure microfluidics as it is tolerant of high pressure. In this PhD thesis, the chips used for acoustic manipulation were made in silicon as silicon works well with standing BAWs.

In Paper III, a PDMS chip is used to collect droplets for time lapse imaging. In Paper IV, a 3D printed chip with micropillars made by photosensitive resin is used to trap droplets for time lapse imaging.

4.1.2 Photolithography

Photoresists are a group of photosensitive polymers where the solubility in the developer can be changed by ultraviolet (UV) exposure. The liquid photoresists can be spin-coated on a silicon wafer and the thickness can be controlled by the spin speed. The viscous photoresist prepared at a low spin speed results in a thick layer. Low spin speeds also have the risk of generating an uneven surface, and there are thick dry films of photoresist that can be directly laminated on the silicon wafer instead. Soft baking is used to evaporate the solvent in the photoresist. The photoresist can be selectively UV exposed by a photomask that contains opaque patterns on a transparent substrate. The photomask can be patterned in a layer of chrome on glass with a high resolution (sub μm). As an alternative, cheaper photomasks with a lower resolution can be prepared by printing the pattern on a plastic substrate by a high-resolution printer. Some photoresists require post-exposure baking as the high temperature will continue to promote the cross-linking reaction. The photoresist can be selectively dissolved in a developer. A positive photoresist that is insoluble in the developer will become soluble after the UV exposure. In contrary a negative photoresist will become insoluble after UV exposure (Figure 22).

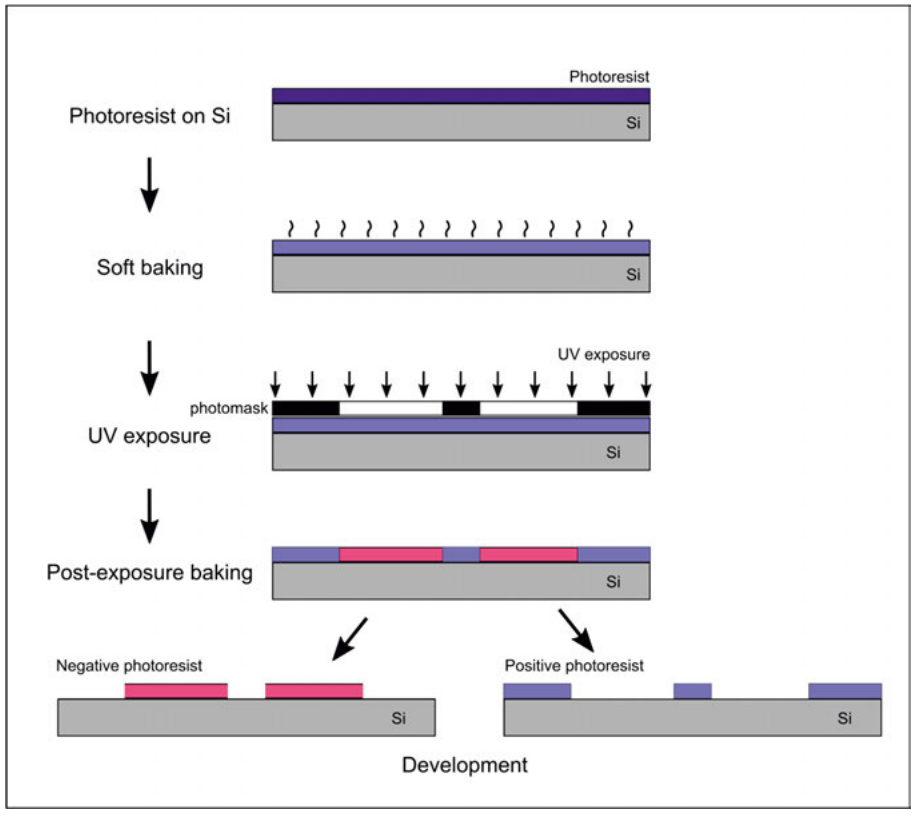

Figure 22 Schematic of the photolithography process.

The resolution of photolithography depends on the light source, the photoresist, the substrate, the photomask, the equipment and the surrounding environment. The typical resolution of UV lithography is 1 µm. There are more advanced technologies used for lithography to overcome the size limitation or the 2D-structure limitation. For example, electron-beam lithography can be used to fabricate nanostructures as the wavelength of the electron-beam (0.01 nm) is much less than that of the UV (365 nm)[99]. Digital micromirror devices (DMD) consisting of an array of micromirrors can be used for 3D printing without the need of photomask[100] and it has been demonstrated to photopolymerize multiple hydrogels simultaneously, used for e.g. single-cell encapsulation.[101] Two-photon lithography can be also used for 3D printing and the efficiency can be increased when working with the DMD.[102]

4.1.3 PDMS chip

PDMS is the most popular material in microfluidics since PDMS has good optical properties for microscopy, high gas permeability and low

autofluorescence.[103] Moreover, PDMS-based chips work well with cells as PDMS is biocompatible. Soft lithography is the standard method to fabricate PDMS chips and the process consists of master fabrication and PDMS casting.

(1) Master fabrication

The master can be fabricated by photolithography of SU-8, a negative photo-resist with high Young's modulus (2 GPa) and high softening point (200 °C). After development, another baking step is often performed at 150 °C for 30 min to eliminate cracks and achieve better mechanical robustness.

Besides SU-8 photolithography, laser machining and cutter plotters can also be used to fabricate masters in thin plastic films. Those methods do not require cleanroom environment or designed masks. Cost and time are saved due to the fast process and cheap materials. However, rough edges and poor resolution limits the usage of these tools for precise structures.

(2) PDMS casting

To prevent PDMS adhering to the master during curing, the master first needs a hydrophobic treatment by trichloro(1H,1H,2H,2H-perfluorooctyl)silane. PDMS is prepared by mixing PDMS base with PDMS curing agent, and after that the PDMS is vacuumed in a dessicator to remove bubbles. Then PDMS is poured on the master and put in an oven, typically at 65°C for 1 hour. After PDMS curing in the oven, the PDMS will replicate the structures from the master when it is peeled from the master. The PDMS is then cut into designed size and holes can be punched to form inlets and outlets. The PDMS channel can be closed by covalent bonding with a glass slide or another PDMS slab (Figure 23). For droplet generation, the channel should be hydrophobic, which is achieved by treating the channel with Sigmacote (a solution of a chlorinated organopolysiloxane in heptane) before use.

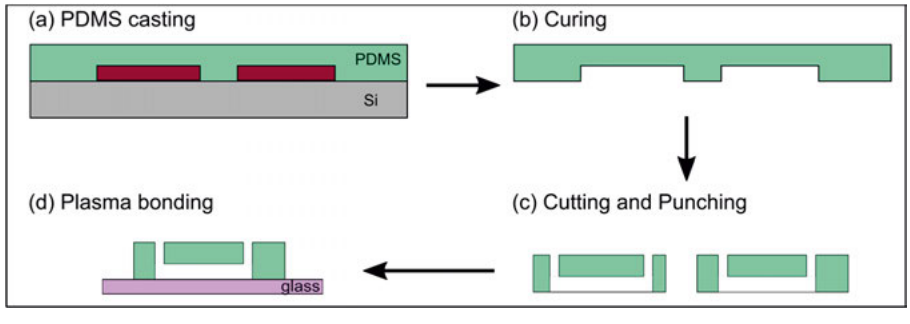

Figure 23 Schematic of the PDMS casting process.

4.1.4 Etching techniques

Photolithography is the first step to define a pattern on the silicon wafer so that the patterned photoresists protects the underneath silicon in a following etch step. Silicon can be etched by a liquid solution, a process called wet etching or by reactive ion plasma, that is called dry etching.

(1) Wet etching

Wet etching uses liquid chemicals to etch the substrate by chemical reactions and it can be categorized into isotropic etching or anisotropic etching according to the etching directionality. Silicon etched in a mixture of nitric acid (HNO_3), hydrofluoric acids (HF) and acetic acid (CH_3COOH) has round cross-section as the silicon is isotopically etched with the same etch rate in all directions (Figure 24a). If a single crystal silicon wafer is etched in potassium hydroxide (KOH), the etching rate in the <100> and the <110> planes is much faster than that in the <111> plane. The anisotropic etching can generate trapezoidal channels as the etching stops at the <111>-plane sidewall (Figure 24b). If the wet etching continues, trapezoidal channel will become V-grooved and then the etching will stop spontaneously. It is possible to generate rectangular channels by using the <111> planes as the sidewalls (Figure 24c). Wet etching is suitable for mass production and it does not require complicated instruments or vacuum system. However, wet etching needs dangerous chemicals such as HF and HNO_3. To obtain vertical sidewalls, specific orientation of the silicon wafer is required which makes it hard to design arbitrary channels with vertical sidewalls using wet etching.

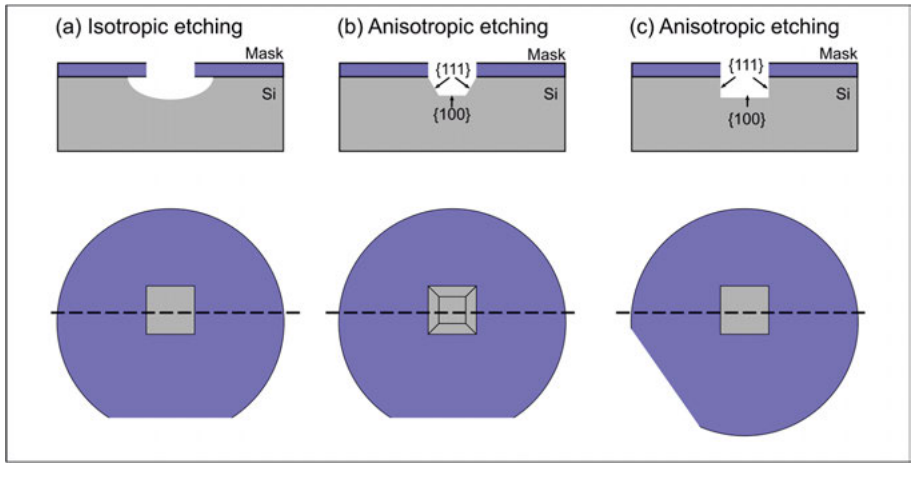

Figure 24 The isotropic wet etching generates (a) round cross-section channel, the anisotropic wet etching generates (b) trapezoidal cross-section channel and (c) rectangular cross-section channel.

(2) Dry etching

Dry etching uses reactive ions to etch the substrate in a vacuum chamber where the generated gas will be pumped away. Deep reactive ion etching (DRIE) is commonly used for microfluidic fabrication as it can etch deep structures with a high etching rate. Moreover, it can generate vertical sidewalls regardless of the orientation of the wafer or the design of the channels.

In this thesis, DRIE is used to fabricate the microfluidic channels with vertical sidewalls for standing BAW generation. Often, the Bosch process is used in DRIE to obtain side walls with a high aspect ratio (Figure 25). The Bosch process contains many isotropic etching steps where each step etches only about hundreds nanometres of silicon.[104] Each etching step starts with supply of octafluorocyclobutane (C_4F_8) and a protective layer is deposited on the silicon wafer. Then oxygen (O_2) is supplied and only the horizontal protective layer is removed. Sulfur hexafluoride (SF_6) is supplied to etch the exposed silicon while the sidewalls are protected by the C_4F_8. By repeating the etching steps, channels with vertical sidewalls are generated and the depth of the channel can be controlled by the number of etching steps or the total etching time. The Bosch process-based dry etcher needs a series of complicated systems, such as a precise control system for gas supplements, a cooling system and a robust vacuum chamber for plasma generation.

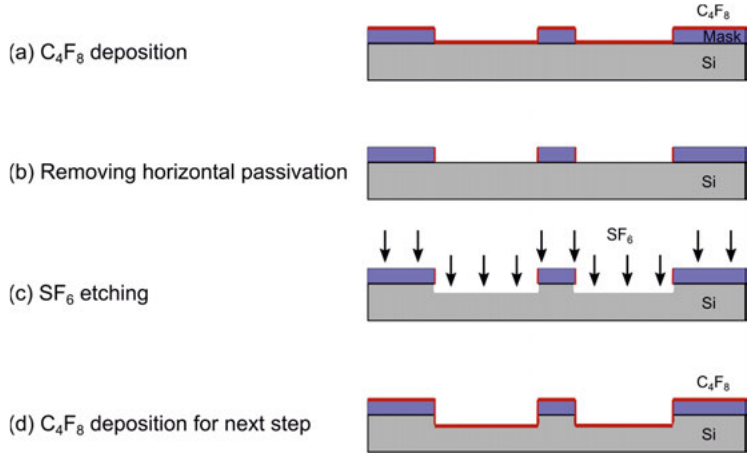

Figure 25 Schematic of a silicon wafer etched by DRIE following the Bosch process.

4.1.5 Additional techniques

After etching, the microfluidic chip also needs other components for active manipulation to be added. For example, the acoustofluidic chip needs the piezoelectric transducer coupled on-chip and the pico-injection needs electrodes.

(1) Electrodes

Electrodes are important components for microfluidics with electrical control. For instance, electric power is applied on electrodes for dielectrophoresis[60] and electrical signals can be measured for electrochemical impedance spectroscopy.[105] In microfluidics, evaporation and sputtering can be used to deposit a thin film of metal on substrate to form the on-chip electrodes. However, evaporation and sputtering need another photolithography step to pattern the electrodes after etching the microfluidic channels.

Integrated electrodes are also needed for droplet electrocoalescence at the pico-injection and for this, metal with a low melting point can be injected into patterned channels to form the electrodes. In this way, channels for flow and electrodes can be integrated in the same design and fabricated at the same time. In Paper I, a liquid alloy (Galinstan) was injected in the electrode channels at the pico-injector. Galinstan is however hard to clean if it is leaked out of the channel and in Paper III and V a different approach was used. Here, the chip was instead heated on a hotplate and a low-temperature solder with melting point of 70 °C was injected into the electrode channels. The melted solder solidifies at room temperature. In this thesis, the electrodes at the pico-injection directly contact the silicon substrate, so high-resistivity silicon wafers (>20,000 Ω·cm) were used to fabricate the acoustic chips to prevent short circuits.

(2) Anodic bonding & assembly

The etched channels can be sealed by anodic bonding with a borosilicate glass wafer, Borofloat® 33. The silicon wafer and the borosilicate glass wafer should be cleaned and activated by piranha solution (a mixture of H_2SO_4 and H_2O_2). The silicon surface is covered by the borosilicate glass wafer and these are put into contact on a hotplate at 380 °C as the silicon and the borosilicate glass have similar thermal expansion at 380 °C. An electrostatic potential of 500V to 1000V is applied on the silicon wafer and borosilicate glass wafer to form the anodic bonding. The silicon/glass wafer is diced into individual chips after anodic bonding. Short pieces of silicone tubing are glued onto the inlets and outlets as connectors and the low temperature solder is injected into the electrode channels. A piezoelectric element is glued onto the silicon chip using cyanoacrylate glue (Figure 26). In paper I, II, III and IV, the piezoelectric element with the primary acoustic frequency of 2 MHz was used to match the channel width of 380 μm. In paper V, a piezoelectric element with the primary acoustic frequency of 5 MHz was used to match the channel width of 150 μm. Repel-Silane (a solution of dimethyldichlorosilane in octamethylcyclooctasilane) was injected into the silicon channels for hydrophobic treatment before use.

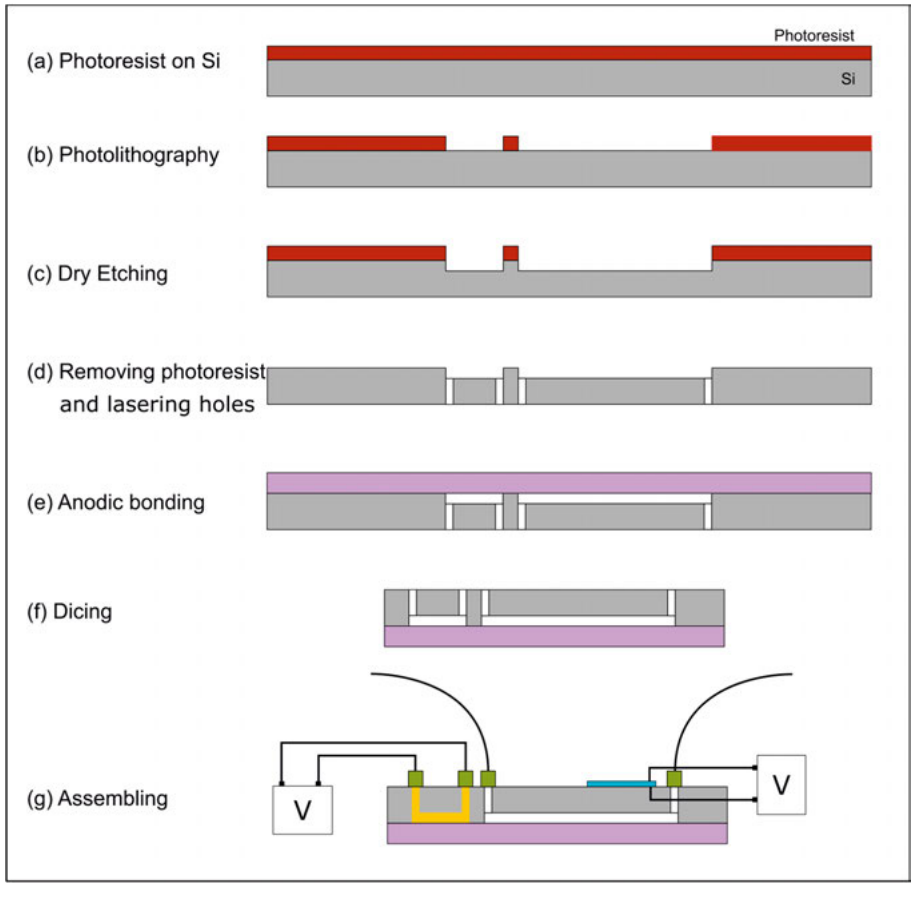

Figure 26 Schematic of the silicon chip fabrication process.

4.2 Experimental setup

To inject the fluids used to form the droplets, syringe pumps are used. The flow rates of each pump can be controlled by a computer. The electrodes for the pico-injector and the piezoelectric element were connected to a function generator. Two signals for pico-injector and piezoelectric element were amplified by two power amplifiers as the required voltages were higher than the maximum output of the signal generator (20 V_{pp}). An oscilloscope was used to monitor the applied signals. The silicon chip was mounted on a chip holder with electrode connectors made by a printed circuit board. The outline of the chip holder is 80mm× 55mm and that fits the stage of the fluorescence microscope and images could be capture through a colour camera (Figure 27).

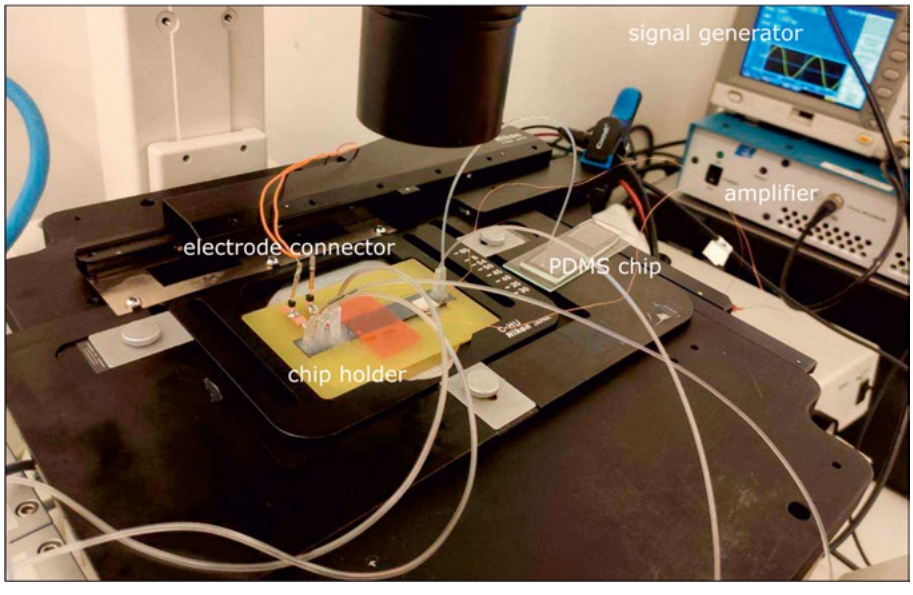

Figure 27 Experimental setup.

Another fluorescence microscope with automatic stage was used for off-line analysis in Paper III and time-lapse imaging in Paper IV and V.

4.3 Measurements

4.3.1 Droplet volume

The images captured by the optical microscope of the droplets only contain two-dimensional top-view information. Hence there are some methods to estimate the droplet volume by the two-dimensional size. For small droplets, the volume of droplets can simply be calculated by $V = \pi HL^2/4$ (spherical droplets) or $V = \pi L^3/6$ (pancake droplets) respectively. For large plug-shaped droplets in a channel, the volume of the droplets (V) is calculated by Equation 4.1[106]:

$$V = \left[HW - (4-\pi)\left(\frac{2}{H} + \frac{2}{W}\right)^{-2}\right]\left(L - \frac{W}{3}\right) \tag{4.1}$$

where H is the height of the channel, W is the width of the channel and L is the length of the droplet.

4.3.2 Fluorescence intensity

In Paper I, a fluorescein solution was used as the dispersed phase for the droplet generation as it is easy to find the outline of the fluorescent droplets by an image analysis software, ImageJ.[107] The volume of each droplet was calculated by Equation 4.1. In Paper III, the fluorescent product of the enzyme reaction was quantified off-chip using a fluorescence microscope. The fluorescence intensity was measured by another image analysis software, CellProfiler.[108] Fluorescein solutions with a known concentration was used to calibrate the relation between the fluorescence intensity and the fluorescein concentration, so that the fluorescence intensity could be used as the read-out of the concentration of the product.

4.3.3 Particle/cell counting

Fluorescent polystyrene beads were used to quantify the particle recovery and enrichment by acoustic focusing. In Paper I and II, fluorescent beads were encapsulated in the droplets and manually counted from fluorescent images as the droplets flowed through the microfluidic channel. Images were collected right before the droplet split and after the droplet split to quantify the enrichment. In Paper V, cells encapsulated in the droplet were imaged in bright field every hour to quantify the cell growth in droplets.

5. Summary

Paper I On-chip background dilution in droplets with high particle recovery using acoustophoresis

This paper presents a droplet microfluidic chip for droplet washing. 10 µm fluorescent polystyrene beads were encapsulated in the droplets and the droplets were split into three daughter droplets at a channel trifurcation. Beads were focused into the centre daughter droplet by acoustophoresis. Then the centre daughter droplet could be injected with fresh fluid via pico-injection. When droplets flowed through this chip, the droplet background could be diluted with high bead recovery.

Light mineral oil with 2% Span 80 was injected as the continuous phase and fluorescent solution containing 10 µm polystyrene beads was injected as the dispersed phase. The droplets were generated on chip and flowed to be split into three daughter droplets at the trifurcation channel. The droplet split ratio was controlled by the withdrawal flow rate of the side channels at the trifurcation channel. Another glass syringe filled with clean water was connected to the pico-injector and clean water was injected into droplets using a syringe pump. At the end of the chip, the outlet was open to the air (Figure 28). To generate the standing BAWs, sine waves with an amplitude of 23 V_{pp} and a frequency of 1.81 MHz were applied over the piezoelectric element. Square waves with an amplitude of 78 V_{pp} and a frequency of 5 kHz were applied on the electrodes for the pico-injection.

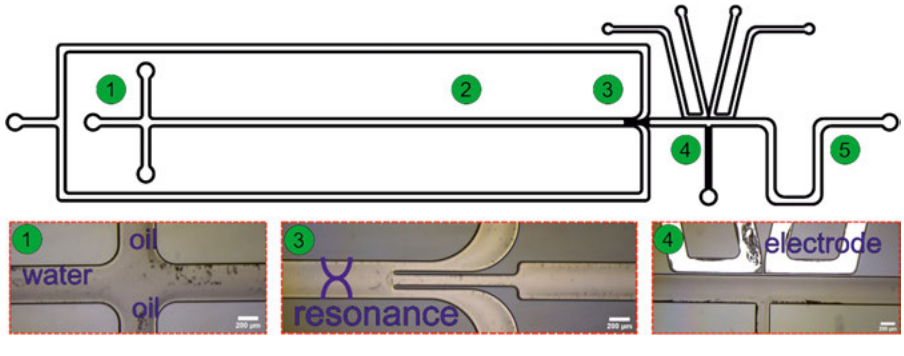

Figure 28 The design of the chip. The chip contains five different unit operators: 1- droplet generation, 2- acoustic focusing, 3- droplet split, 4- pico-injection and 5- serpentine mixing. Reprinted with permission from ref. 88. Copyright 2019 American Institute of Physics.

The capability of the pico-injection was characterized by varying the flow rate of the pico-injector. The abilities of dilution and bead recovery were characterized by varying the droplet size, the total flow rate and the droplet split ratio. This microfluidic system could achieve a maximum 4.3-fold background dilution (from 1.00 mg/ml to 0.23 mg/ml) with a bead recovery of 87.7% (Figure 29a). Moreover, we succeeded in applying this chip to performing a droplet wash step with encapsulated cells at high cell recovery (Figure 29b).

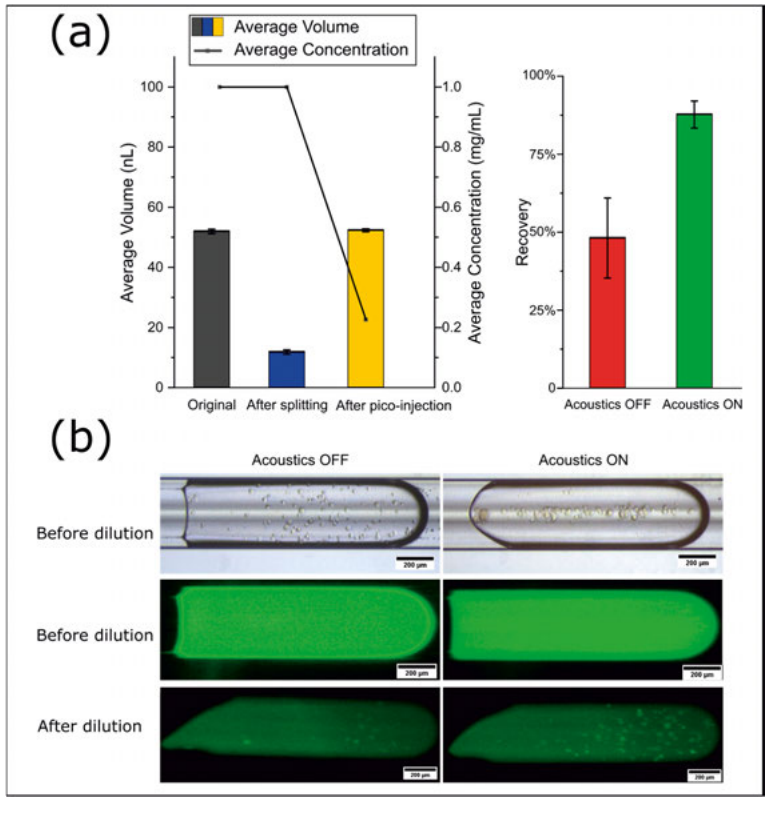

Figure 29 (a) Left: The maximum droplet dilution. The grey bar represents the volumes of the original droplet, the blue bar represents the droplets after the split, and the yellow bar represents after the pico-injection. Right: The recovery of beads after droplet split without (red) and with (green) acoustic actuation at the maximum droplet dilution. Error bars represent the standard deviation. (b) Optical images of droplets with encapsulated endothelial cells taken in bright field and fluorescent mode before droplet dilution and after droplet dilution. Reprinted with permission from ref. 88. Copyright 2019 American Institute of Physics.

Paper II Optimisation of the droplet split design for improved acoustic particle enrichment in droplet microfluidics

This paper explores the improvement of particle enrichment in droplets by optimising the droplet split channel design. This chip contains droplet generation, acoustic focusing and droplet split (Figure 30). The particle recovery and enrichment were characterized by different split channels, actuation voltages of the piezoelectric element and flow ratios between the centre and side outlet split channels.

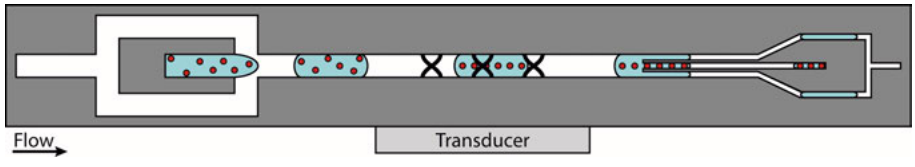

Figure 30 The microfluidic chip for particle enrichment in droplets. Reprinted with permission from ref. 59. Copyright 2020 Elsevier.

The droplets are split at trifurcation channels (Figure 31), and the dimensions of the three droplet splits are presented in Table 3. Water containing fluorescent polystyrene microbeads (3.2 µm, 4.8 µm or 9.9 µm diameter) was used as the dispersed phase, and light mineral oil with 1% Span 80 was used as the continuous phase. The flow rates for droplet generation were set to constantly generate droplets of 30 nL. The droplet split ratio between the centre and side outlet channels was controlled by the withdrawal flow rate at the side split channel. The piezoelectric element was actuated to generate the standing BAWs in the channel. The actuation frequency was optimized for each chip and the actuation voltages were set to be 5V, 7.5V and 10V. When the droplet was split into three daughter droplets, the particles were focused into the central daughter droplet by acoustics, otherwise the particles were randomly distributed in the three daughter droplets (Figure 32).

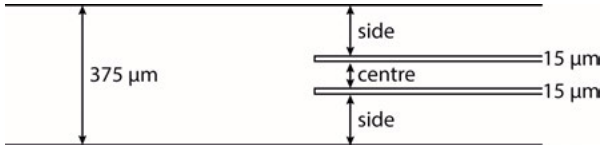

Figure 31 Design of trifurcation channels for droplet split. Reprinted with permission from ref. 59. Copyright 2020 Elsevier.

Table 3. Dimensions of the three droplet splits. Reprinted with permission from ref. 59. Copyright 2020 Elsevier.

	Width of centre outlet channel (μm)	Width of each side outlet channel (μm)
Chip A	115	115
Chip B	57	144
Chip C	38	153

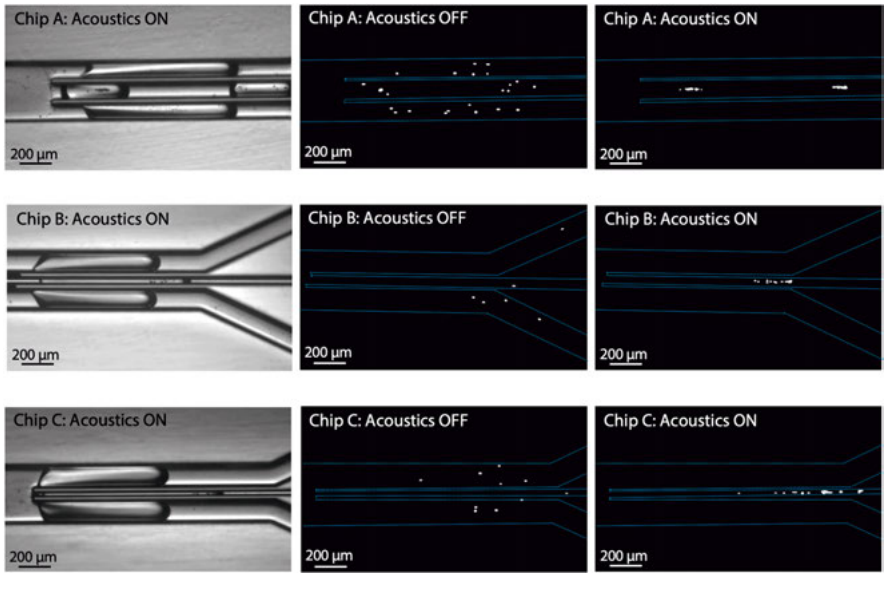

Figure 32 Droplet splitting and acoustic particle enrichment in the three different droplet split designs. Reprinted with permission from ref. 59. Copyright 2020 Elsevier.

When the centre outlet flow rate was set to 1.0 μL/min and the total side outlet flow rate was set to 5.0 μL/min, the particle recovery increases as the actuation voltage increases and it reaches 100% at 10V for all three chips. As the centre outlet flow rate decreased, all three chips showed a decreasing trend of particle recovery and an increasing trend of particle enrichment. Chip C that has the smallest width of the centre outlet channel showed higher enrichment than the other chips. Chip C was also used to demonstrate focusing of particles of different sizes (3.2 μm, 4.8 μm and 9.9 μm diameter polystyrene particles).

Paper III A droplet acoustofluidic platform for time-controlled microbead-based reactions

This paper presents a droplet acoustofluidic chip for time-controlled reactions that can be combined with off-line optical readout. The enzymatic conversion of fluorescein diphosphate (FDP) to fluorescein by alkaline phosphatase (ALP) was demonstrated by this chip and the time of the enzymatic reaction could be controlled by physically removing the enzyme-coupled microbeads from the droplets.

Polystyrene microbeads with diameter of 5 μm were coupled with ALP via streptavidin-biotin binding before use (Figure 33a). Droplets containing FDP substrate were generated on the chip and ALP-coupled microbeads were added into the droplets via pico-injection. The reaction started as soon as the enzyme/microbead complexes were added, and the reaction was stopped when the microbeads were separated from the droplets at the bifurcation channel. The encapsulated microbeads were focused in the droplets by acoustophoresis during the sampling to make sure no beads were drawn into the side daughter droplets collected for off-line analysis. The three side outlet channels were placed in series along the main flow channel and they were used independently for sampling from the droplets (Figure 33b). The time of the reaction could be controlled by using different outlets at the same flow rates. The enzymatic conversion could be measured with fluorescence read-out in the collected droplets in a separate PDMS chip mounted in a microscope (Figure 33c).

For droplet generation, light mineral oil with 3% PGPR was used as the continuous phase and 10 μM FDP in diethanolamine (DEA) buffer was used as the dispersed phase. The enzyme-coupled microbeads in DEA buffer was injected into the droplets via the pico-injector. For each droplet split, the collected droplets from each split channel with acoustics showed a lower fluorescent intensity than that without acoustics, indicating that the reaction time could be controlled by the channel length with acoustics. The collected droplets with or without acoustics applied were detected for 30 min at intervals of 6 min. The DEA buffer was injected into droplets containing FDP through the pico-injector as controls. The fluorescein concentration in the droplets without acoustics was increasing drastically while the fluorescein concentration in the droplets collected with acoustics was increasing only slightly (Figure 34). With acoustics, the product in collected droplets can be constant and it is suitable for off-line analysis.

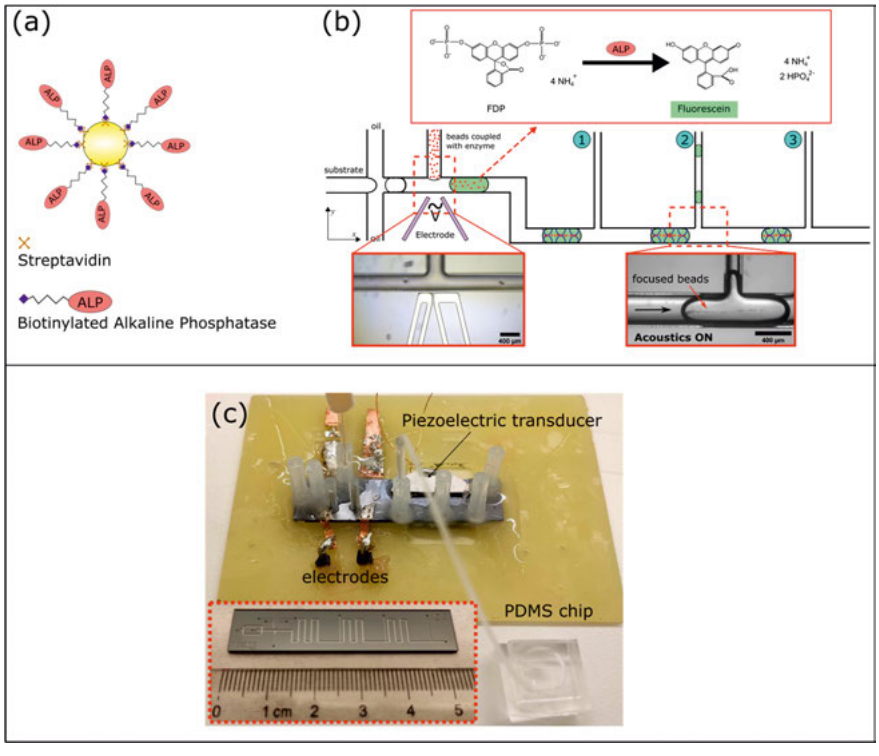

Figure 33 (a) Schematic drawing of the streptavidin bead coupled with biotinylated ALP. (b) The chip contains droplet generation, pico-injector and three droplet splits. The 5 µm microbeads can be focused in the centre of the droplet by standing bulk acoustic waves. The length of the reaction channel is not according to scale. (c) The image shows the tubing connection for droplet transfer between the silicon chip and the PDMS chip. Reprinted with permission from ref. 23. Copyright 2021 American Institute of Physics.

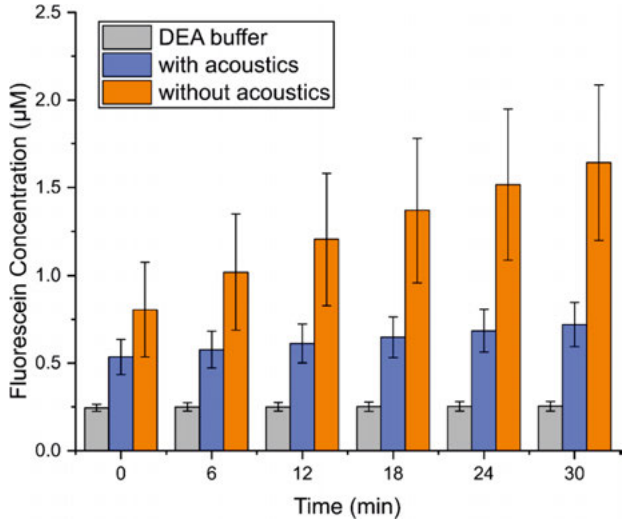

Figure 34 Fluorescein concentration in droplets collected at split 3 with or without acoustics applied. Data shows how the concentration varied over 30 min. (For the DEA buffer, R^2=0.843; for the FDP with acoustics, R^2=0.999; for the FDP without acoustics, R^2=0.991.) Reprinted with permission from ref. 23. Copyright 2021 American Institute of Physics.

Paper IV Mapping the acoustic properties of two-phase systems for use in droplet acoustofluidics

This paper investigates the acoustic properties, *i.e.* speed of sound and density, of selected oils that can be used as the continuous phase in droplet microfluidic systems. A droplet microfluidic system where the phases have similar acoustic properties can obtain high-quality acoustic focusing inside the droplets.[46] This paper continues to investigate acoustic properties of more hydrocarbon oils. A silicone oil and two fluorinated oils are also tested as references.

Speed of sound and density of nine different oils were measured at 25 °C and 37 °C respectively: 1) hydrocarbon oils (light mineral oil, heavy mineral oil, linseed oil, sunflower oil, olive oil, food oil (75% rapeseed oil + 25% sunflower oil)), 2) fluorinated oils (FC-40, HFE-7500), and 3) silicone oil 50 cSt. The experimental results show that within our collection, hydrocarbon oils show matched acoustic properties of water, silicon oil shows mismatched characteristic acoustic impedance of water and fluorinated oils show mismatched speed of sound of water (Table 4).

Table 4. Density, speed of sound and acoustic impedance of a selection of oils at 25 and 37℃ respectively as compared to DI water. (The unit of the acoustic impedance is Rayl: 1 Rayl = 1 kg m^{-2} s^{-1}.)

Fluid	Density at 25℃ (kg m^{-3})	Speed of sound at 25℃ (m s^{-1})	Characteristic acoustic impedance at 25℃ (MRayl)	Density at 37℃ (kg m^{-3})	Speed of sound at 37℃ (m s^{-1})	Characteristic acoustic impedance at 37℃ (MRayl)
DI water	997.0	1496.7	1.49	993.4	1523.6	1.51
Light mineral oil	844.9	1428.2	1.21	838.4	1387.5	1.16
Heavy mineral oil	858.9	1487.6	1.28	852.0	1412.1	1.20
Olive oil	910.2	1458.6	1.33	903.5	1421.2	1.28
Linseed oil	925.2	1461.9	1.35	918.8	1428.3	1.31
Sunflower oil	915.4	1457.6	1.33	907.8	1420.8	1.29
Food oil	915.9	1463.4	1.34	908.2	1424.9	1.29
Silicone oil	959.6	1045.9	1.00	950.3	1012.4	0.96
HFE-7500	1618.4	709.9	1.15	1594.8	674.4	1.08
FC-40	1865.6	687.3	1.28	1841.8	653.7	1.20

The fluorescein solution with a concentration of 0.0 2mg/mL was used as the dispersed phase and the selected oils were used as the continuous phase. The fluorescent droplets were generated at the same flow rates in a silicon chip (Figure 35). The droplets generated in light mineral oil shows the highest

fluorescence intensity. When the surfactant (Span 80, EM 90 and PGPR) was added in light mineral oil to generate droplets at the same flow rates, the droplet volume was decreased due to the lower interfacial tension and the fluorescence intensity was also decreased.

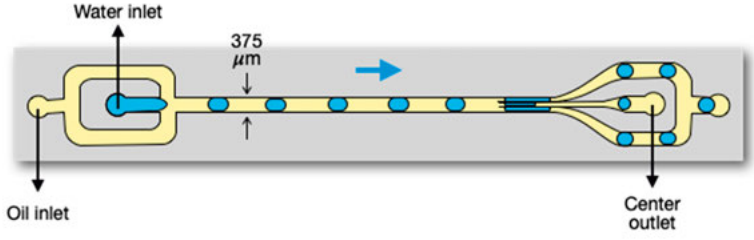

Figure 35 A silicon chip design for droplet acoustophoresis.

The 5% PGPR was added in other hydrocarbon oils as the continuous phase to generate droplets. The generated droplets were transferred onto a PDMS chip for fluorescence intensity measurement in 15 min and 30 min (Figure 36). The fluorescence intensity in droplets decreased with time, and the reason could be photobleaching and molecular diffusion across the droplets. The droplets generated by light mineral oil with 5% PGPR show constant fluorescence intensity, and also good stability when sudden pressure change occurs due to disconnecting tubing from the PDMS chip.

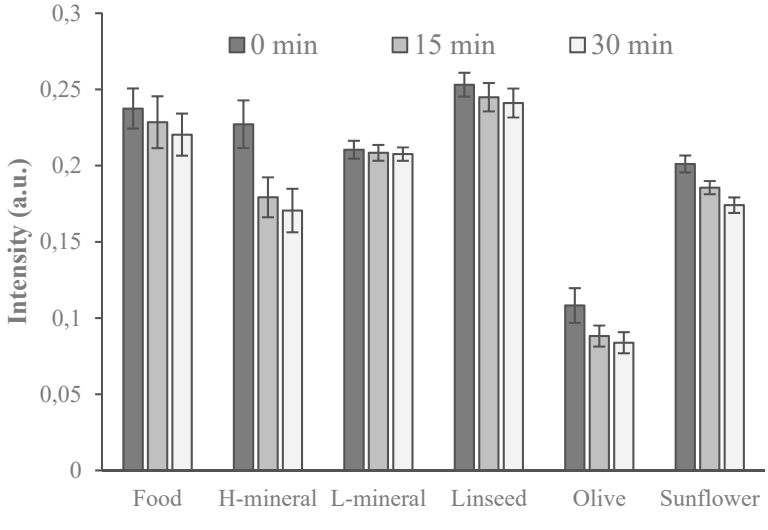

Figure 36 The fluorescence intensity in droplets generated by hydrocarbon oils with 5% PGPR.

Paper V Long-term droplet cell culture enabled by droplet acoustofluidics

This paper presents a droplet platform to exchange in-droplet cell medium, which contains the pico-injection and droplet split with acoustophoresis (Figure 37). This droplet platform can be used for long-term cell culture. The piezoelectric element with primary frequency of 5 MHz was used to generate BAWs so that the channel width was designed as 150 μm to match the acoustic frequency of the half wavelength resonance.

In this paper, yeast cells were suspended in phosphate buffered saline (PBS) mixed with 10% cell medium. The cell concentration adjusted to 10^6 /mL was used as the dispersed phase and the light mineral oil with 3% PGPR was used as the continuous phase. The PBS mixed with 10% cell medium was injected to the pico-injector. Yeast cells were encapsulated in droplets by a PDMS chip and the generated droplets were collected in a syringe prefilled with the continuous phase for cell culture. The droplets were loaded on a glass chip to be trapped in an array of 3D printed pillars and a microscope with a time-lapse camera was used to record the cell number in the droplets.

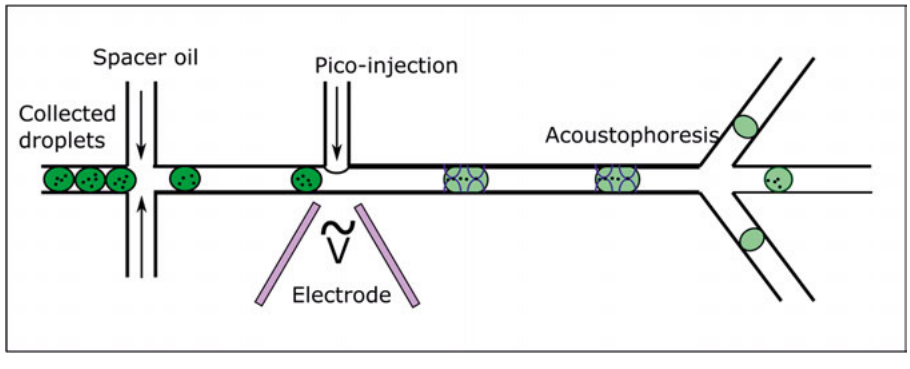

Figure 37 The chip design for exchanging cell medium in droplets.

After droplet generation, yeast cells in droplets continued to divide in the first 8 hours and then reached the stationary phase. The droplets collected in a syringe were reinjected into the chip to exchange the cell medium after 6 hours and 8 hours cell culture in syringe. The droplets were loaded on the glass chip after got cell medium exchanged by this chip. The cell number in droplets was continued to be recorded. After exchanged the cell medium in droplets, the cells are able to divide again but they will also reach the second stationary phase soon (Figure 38).

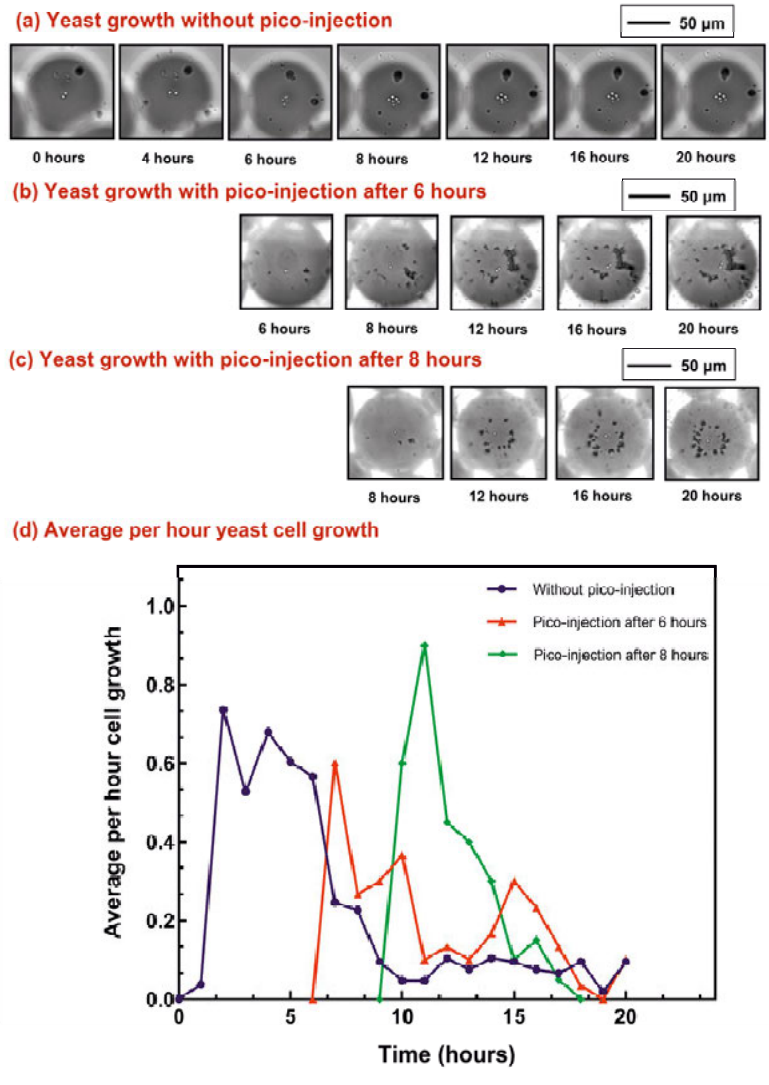

Figure 38 (a) Images to show the cell growth in droplet without pico-injection. (b-c) Images to show the cell growth in droplet with pico-injection. (d) Average cell growth in droplet every hour without medium exchange and with medium exchange after 6 and 8 hours, respectively.

6. Conclusion and outlook

Droplet microfluidics has been growing drastically during the past years. Since the size of droplets is at the microscale, it is hard to manipulate the droplets by conventional methods. This thesis presents a general method to manipulate particles inside droplets by the combination of the pico-injection and the droplet split with acoustophoresis.

The first study demonstrated at system that could be used to wash droplets by diluting the background signal without losing the encapsulated particles via acoustophoresis and pico-injection. The results showed the capability of this chip to perform background dilution in droplets with a large range of volume and flow rates. This microfluidic system could achieve a maximum 4.3-fold background dilution (from 1.00mg/ml to 0.23mg/ml) with a particle recovery of 87.7%. Moreover, this chip was successfully applied to perform background dilution in droplets with encapsulated cells at high cell recovery.

Particle enrichment is a common step for biochemical assays. The droplet split design could be optimized to improve the particle enrichment in the droplets. The results showed the maximum enrichment was achieved on the chip with the narrowest centre channel at the split. It has been demonstrated to work for smaller particles with diameter of 3.2 μm.

For biochemical reactions in droplets, the reaction product confined in the droplets requires on-chip detection. The third study presented a proof-of-concept applications to use this system for time-controlled reactions, where the generated enzymatic product could be quantified via off-line analysis. The reaction time was controlled by the flow rates and the position of the split channel. Moreover, the separated droplets were collected on another PDMS chip for off-line measurement as the reaction stops when the enzyme-coupled beads were sorted out by acoustophoresis.

In the fourth study, droplets were generated by different oils and the acoustic properties of a selection of fluids were mapped. Hydrocarbon oils showed matched acoustic properties with water, and that is required to form strong standing BAWs in droplets. PGPR was the surfactant added in hydrocarbon oils and that could stabilize droplet generation.

The fifth study presented another application for cell culture. Here, the total culture time of yeast cells was extended by refreshing the culture media inside the droplets.

This platform is expected to take part in more biochemical applications. Long-term cell culture can be formed by this platform and that can be used for tissue engineering. For example, the 3D spheroid can be formed from a seeding cell in droplet and it can mimic the *in vivo* microenvironment for drug delivery test. Another application is in-droplet disease diagnosis. Rare gene mutations can be detected after gene amplification by ddPCR. Screening, including gene screening and drug screening can be performed in droplet with high throughput. Drugs or other stimuli can be added into a library of droplets via the pico-injection and the supernatant solution can be separated from the droplets for different types of off-line analysis such as fluorescence plate reader or mass spectrometry. It can be used to screen the drug with best performance.

However, it is necessary to consider the ethics when performing biochemical assays. For example, the gene screening can also be used to screen the mutated genes with high drug resistance that could be a threat to the balance of nature. The muted bacteria with high antibiotic resistance can be screened when exposed to antibiotics, and antibiotic misuse can cause life-threatening infections. It is important for researcher to consider the ethical effect that could raise from gene screening or drug screening.

Popular scientific summary

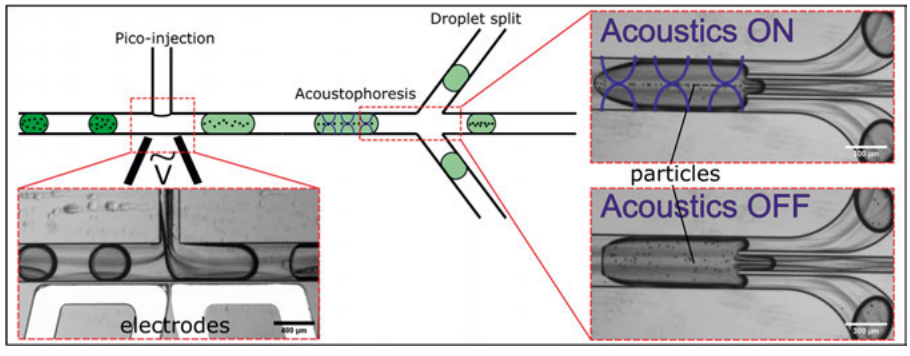

Figure 39 Schematic to show the droplet washing by pico-injection and droplet split with acoustics.

Microfluidics is a technology to manipulate fluids at a microscale chip. The microfluidic chip has the same functions as the functions that can be performed in a conventional lab, so it is also called “Lab on a Chip”. Water-in-oil droplets can be generated on a microfluidic chip, and the individual droplets can work as very small reaction vials. A large number of droplets can be generated in a short period of time and the sizes of droplets are highly monodispersed. The droplets are separated from each other by the oil phase, and the droplets can be used to perform thousands of reactions in parallel. Droplets can be used as microscopic containers for biochemical applications, and that is advantageous as it allows for fast reactions with the use of less reagents.

In the conventional lab, exchanging cell medium or washing cells can be performed by removing the supernatant after centrifugation and adding fresh medium. However, it is challenging to perform this in droplets as they are too small. This thesis presents a microfluidic chip to wash the background in droplets. This chip contains pico-injection and droplet split with acoustics (Figure 39). The pico-injection can be used to add fresh medium into existing droplets. Acoustic waves are generated by a piezoelectric element attached on the silicon chip and the waves propagate to the channel. When the channel width is equal to the half wavelength of the acoustic waves, standing waves can be formed in the silicon channels. Particles will be moved to the nodes or antinodes of the standing waves. Here, the channel width is 375 µm and that matches the frequency of acoustic waves at 2 MHz so that standing waves can

be formed in the channels. Polystyrene beads and cells will move to the node of the standing waves which is located along the centre-line of the channel. After droplet split, all particles will flow into the same daughter droplet and the supernatant of the original droplets can be removed. By this way, the droplets can be washed on this chip. With the same method, cell medium in droplets containing cells can be exchanged.

Particles can be focused in droplets by the acoustics, but the geometry of the droplet split will also affect the particle distribution in the daughter droplets. In the second study, the droplet split design was optimized to improve the enrichment of particles into the same daughter droplet.

In another study, the acoustic properties (i.e. density, speed of sound) of oils are measured, and the effect of the oil on the particle focusing in droplets is evaluated by experiments.

This microfluidic chip can also be used to control reactions in droplets. In one example, the enzyme reaction starts when enzyme is added into the droplet containing substrate as the enzyme can catalyse the substrate. The enzyme reaction can then be stopped when the enzyme is removed from the droplet with acoustics.

In this thesis, a couple of basic biochemical applications has been implemented by this microfluidic chip. I believe this system can be used for more biochemical assays and I expect it will apply on more specific applications.

Populärvetenskaplig sammanfattning

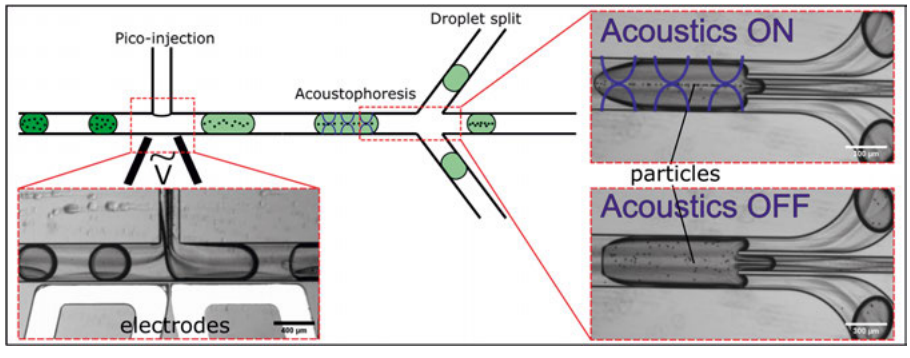

Figur 40 Schematisk bild för att visa dropptvättning genom pico-injektion och droppdelning kombinerat med akustofores.

Mikrofluidik är en teknik för att manipulera vätskor på ett chip i mikroskala. Det mikrofluidiska chippet har samma funktioner som ett konventionellt labb, och brukar också kallas "Lab on a Chip". Vatten-i-olja-droppar kan genereras på ett mikrofluidikchip där varje enskild droppe fungerar som ett provrör. Ett stort antal droppar kan genereras på kort tid och storleken på dropparna är i stort sett identiska. Eftersom dropparna åtskiljs av en olja är de oberoende av varandra och kan därför användas som en plattform för att utföra ett väldigt stort antal analyser parallellt. Droppar kan alltså användas som mikroskopiska behållare för biokemiska analyser, vilket också är bra då det minskar kravet på reagensvolymer.

I det konventionella labbet kan utbyte av cellmedium eller tvättning av celler utföras genom att avlägsna en del av cellmediumet efter centrifugering och tillsätta färskt medium. Detta är dock väldigt svårt att göra i droppar eftersom de är så små, typiskt bara en diameter på ett par hundra mikrometer. Den här avhandlingen presenterar nya tekniker för att kunna utföra dessa steg i droppar. Chippet innehåller en s.k. pico-injektor som kan användas för att tillsätta nytt medium och en kanalsplitt som delar dropparna (Figur 40). När dropparna delas utsätts de samtidigt för ett akustiskt tryckfält som positionerar partiklarna inuti dropparna längs med mitten av kanalen. På det sättet säkerställs att partiklarna inte fördelas jämnt i den delade droppen, utan koncentreras i en specifik dotterdroppe. De akustiska vågorna genereras av ett piezoelektriskt element som är fäst på kiselchippet och fortplantar sig till kanalen. När

kanalbredden är lika med halva våglängden för de akustiska vågorna kan stående vågor bildas i kiselkanalen och partiklarna kommer att flyttas till noderna eller antinoderna av tryckfältet. Här är kanalbredden 375 µm, vilket matchar frekvensen av akustiska vågor på 2 MHz och leder till att kulor i polystyren och celler kommer flyttas till noden av de stående vågorna i mitten av kanalen. Genom att använda samma metod kan cellodlingsmedium förnyas i dropparna så att celler kan odlas i dropparna under längre tid.

Partiklar kan fokuseras i droppar med hjälp av akustiken, men geometrin för droppdelningen kommer också att påverka partikelfördelningen i dotterdropparna. I den andra studien optimerades droppdelningsdesignen för att öka andelen partiklar som fokuseras i samma dotterdroppe.

Oljornas akustiska egenskaper (d.v.s. ljudhastighet och densitet) har också studerats i den här avhandlingen för att identifiera den bästa vatten/olja kombinationen for droppbaserad akustofluidik.

Detta mikrofluidala chip kan också användas för att tidsbestämma kemiska reaktioner i dropparna. I exemplet här, startar en enzymreaktion när enzym som är kemiskt bundet till plastkulor tillsätts i droppar som innehåller enzymsubstrat. Vid bestämda tidpunkter kan sen små prover tas från de olika dropparna för att bestämma effektiviteten av den enzymatiska processen. Genom att akustiskt fokusera plastkulorna i dropparna, säkerställs att endast enzymprodukten tas ut.

I den här avhandlingen har jag visat på ett par grundläggande biokemiska tillämpningar som kan implementeras till den droppbaserade mikrofluidiken med hjälp av integrerad akustik. I framtiden, tror jag att det även kommer kunna fungera för fler biokemiska analyser och jag förväntar mig att se utvecklingen av mer specifika tillämpningar.

Acknowledgements

It is a great journey for me to explore the droplet acoustofluidics in this PhD project. I am very happy to work in Uppsala University during my PhD study. I really appreciate the help and support that I have received from my colleagues, my friends and my family.

First, I would like to thank my supervisor Maria Tenje. Thank you for being my supervisor and supporting my PhD study. I am inspired by your enthusiasm on research. I appreciate your patience and guidance on my research. I have learnt a lot about academic research from supervision meetings and discussions. I would like to thank my co-supervisor Anna for teaching me to fabricate the chips and to build the experimental setup. I appreciate your help of writing and experiment. I would like to thank Laurent for sharing your knowledge on droplet microfluidics. Thanks to Milena for the help of chip fabrication. Thanks to Atena and Sofia for teaching me about electrical measurement. Thanks to Hannah for teaching me about reviewing and writing. Thanks to Qian for your hard working in your master project. Thanks to Susan for organizing everything in the group. Thanks to my lab buddies for your help and company in the cleanroom: Federico, Sarah, Ana Maria, Gabriel, Simon, Karolina, Javier, Abdul, Lulu, Samah, Sofia, Praneeth, Samuel and Sagar. I would like to thank all my colleagues in EMBLA group as you create a wonderful working environment.

I also would like to thank my colleagues at the MST division and the MET division. Thanks to Klas for co-supervising me during my first PhD year and I appreciate the discussion with you. Thanks to Lena for guidance to the actuator lab. Thanks to Hugo for the help of photomask fabrication and CAD drawing. Thanks to Zhigang for introducing me into microfluidics. I would like to thank colleagues for your help in the lab: Klara, Jan, Anton, Erika, Farnaz, Ragnar. I enjoyed the group activities with you, including SciFest, kick-off and weekly fika.

I would like to thank my friends in Ångstrom. Thanks to Qitao, Shuangshuang, Xingxing, Huan, Lei, Tianbo, Shenyang, Pei, Hailiang, Chenyu, Renbin, Yingtao and Yuan Zhu, for the time we celebrated traditional Chinese festivals. Thanks to Bei, Yuan Cui, Jialun, Fengnan, Zhouyuan and Hongyu

for organizing the Mahjong Satuaday Night that made my life interesting in Uppsala. Thanks to my gym friends, Shiyu, Rui, Xueying, Pei, Zheqiang and Jing. Let's go stronger! Special thanks to my fan, A Wei and my neighbour Hao, for your help during my first year of my PhD.

My gratitude also goes to my friends in distance: Wenchao, Xiaoya, Jie and Shuo. I would like to thank my sisters, Wenhua and Wenjing, my cousin, Kunpeng, and my family. I can't complete my PhD degree without your support.

I am grateful for financial support from China Scholarship Council and travel grants from Anna Maria Lundin's Scholarship.

最后，感谢我的家人朋友们一直以来的支持和关心。

Zhenhua

References

1. N.-T. Nguyen, S. T. Wereley and S. A. M. Shaegh, *Fundamentals and applications of microfluidics*, Artech house, 2019.
2. K. J. Land, D. I. Boeras, X.-S. Chen, A. R. Ramsay and R. W. Peeling, *Nature Microbiology*, 2019, **4**, 46-54.
3. S. Battat, D. A. Weitz and G. M. Whitesides, *Lab on a Chip*, 2022, **22**, 530-536.
4. S. Sachdeva, R. W. Davis and A. K. Saha, *Frontiers in Bioengineering and Biotechnology*, 2021, **8**.
5. https://www.researchandmarkets.com/reports/5449009/global-microfluidics-market-by-product-devices).
6. C. Wyatt Shields Iv, C. D. Reyes and G. P. López, *Lab on a Chip*, 2015, **15**, 1230-1249.
7. Y. Chen, P. Li, P.-H. Huang, Y. Xie, J. D. Mai, L. Wang, N.-T. Nguyen and T. J. Huang, *Lab on a Chip*, 2014, **14**, 626-645.
8. D. R. Gossett, W. M. Weaver, A. J. Mach, S. C. Hur, H. T. K. Tse, W. Lee, H. Amini and D. Di Carlo, *Analytical and Bioanalytical Chemistry*, 2010, **397**, 3249-3267.
9. Y. I. Wang, H. E. Abaci and M. L. Shuler, *Biotechnology and Bioengineering*, 2017, **114**, 184-194.
10. Y. Li and E. Kumacheva, *Science Advances*, 2018, **4**, eaas8998.
11. A. Lenshof, M. Evander, T. Laurell and J. Nilsson, *Lab on a Chip*, 2012, **12**, 684-695.
12. M. Andersson, K. Hjort and L. Klintberg, *Journal of Micromechanics and Microengineering*, 2016, **26**, 095009.
13. K. Raj M and S. Chakraborty, *Journal of Applied Polymer Science*, 2020, **137**, 48958.
14. A. Folch, *Introduction to bioMEMS*, CRC Press, 2016.
15. T. M. Squires and S. R. Quake, *Reviews of Modern Physics*, 2005, **77**, 977-1026.
16. J. M. Ottino, S. R. Wiggins, M. R. Bringer, C. J. Gerdts, H. Song, J. D. Tice and R. F. Ismagilov, *Philosophical Transactions of the Royal Society of London. Series A: Mathematical, Physical and Engineering Sciences*, 2004, **362**, 1087-1104.
17. S. L. Sjostrom, H. N. Joensson and H. A. Svahn, *Lab on a Chip*, 2013, **13**, 1754-1761.
18. E. Y. Basova and F. Foret, *Analyst*, 2015, **140**, 22-38.

19. T. S. Kaminski, O. Scheler and P. Garstecki, *Lab on a Chip*, 2016, **16**, 2168-2187.
20. S. Sart, G. Ronteix, S. Jain, G. Amselem and C. N. Baroud, *Chemical Reviews*, 2022, DOI: 10.1021/acs.chemrev.1c00666.
21. K. Choi, A. H. C. Ng, R. Fobel and A. R. Wheeler, *Annual Review of Analytical Chemistry*, 2012, **5**, 413-440.
22. L. Amirifar, M. Besanjideh, R. Nasiri, A. Shamloo, F. Nasrollahi, N. R. de Barros, E. Davoodi, A. Erdem, M. Mahmoodi, V. Hosseini, H. Montazerian, J. Jahangiry, M. A. Darabi, R. Haghniaz, M. R. Dokmeci, N. Annabi, S. Ahadian and A. Khademhosseini, *Biofabrication*, 2022, **14**, 022001.
23. Z. Liu, A. Fornell and M. Tenje, *Biomicrofluidics*, 2021, **15**, 034103.
24. S. L. Sjostrom, Y. Bai, M. Huang, Z. Liu, J. Nielsen, H. N. Joensson and H. Andersson Svahn, *Lab on a Chip*, 2014, **14**, 806-813.
25. C. D. Ahrberg, A. Manz and B. G. Chung, *Lab on a Chip*, 2016, **16**, 3866-3884.
26. S. Olmedillas-López, M. García-Arranz and D. García-Olmo, *Molecular Diagnosis & Therapy*, 2017, **21**, 493-510.
27. M. Deiana, A. Mori, C. Piubelli, S. Scarso, M. Favarato and E. Pomari, *Scientific Reports*, 2020, **10**, 18764.
28. H. N. Vasudevan, P. Xu, V. Servellita, S. Miller, L. Liu, A. Gopez, C. Y. Chiu and A. R. Abate, *Scientific Reports*, 2021, **11**, 780.
29. L. Cohen, N. Cui, Y. Cai, P. M. Garden, X. Li, D. A. Weitz and D. R. Walt, *ACS Nano*, 2020, **14**, 9491-9501.
30. L. Shang, Y. Cheng and Y. Zhao, *Chemical Reviews*, 2017, **117**, 7964-8040.
31. L. L. Lazarus, C. T. Riche, B. C. Marin, M. Gupta, N. Malmstadt and R. L. Brutchey, *ACS Applied Materials & Interfaces*, 2012, **4**, 3077-3083.
32. J. B. Wacker, I. Lignos, V. K. Parashar and M. A. M. Gijs, *Lab on a Chip*, 2012, **12**, 3111-3116.
33. K. Matuła, F. Rivello and W. T. S. Huck, *Advanced Biosystems*, 2020, **4**, 1900188.
34. N. Shembekar, H. Hu, D. Eustace and C. A. Merten, *Cell Reports*, 2018, **22**, 2206-2215.
35. O. J. Miller, A. E. Harrak, T. Mangeat, J.-C. Baret, L. Frenz, B. E. Debs, E. Mayot, M. L. Samuels, E. K. Rooney, P. Dieu, M. Galvan, D. R. Link and A. D. Griffiths, *Proceedings of the National Academy of Sciences*, 2012, **109**, 378-383.
36. A. Fornell, H. Pohlit, Q. Shi and M. Tenje, *Scientific Reports*, 2021, **11**, 7479.
37. A. Sauret, C. Spandagos and H. C. Shum, *Lab on a Chip*, 2012, **12**, 3380-3386.
38. M. He, J. S. Kuo and D. T. Chiu, *Langmuir*, 2006, **22**, 6408-6413.
39. S. Kahkeshani and D. Di Carlo, *Lab on a Chip*, 2016, **16**, 2474-2480.

40. A. Bransky, N. Korin, M. Khoury and S. Levenberg, *Lab on a Chip*, 2009, **9**, 516-520.
41. J. C. Brenker, D. J. Collins, H. Van Phan, T. Alan and A. Neild, *Lab on a Chip*, 2016, **16**, 1675-1683.
42. P. Zhu and L. Wang, *Lab on a Chip*, 2017, **17**, 34-75.
43. R. Dangla, F. Gallaire and C. N. Baroud, *Lab on a Chip*, 2010, **10**, 2972-2978.
44. M. C. Davis, P. W. Fedick, D. V. Lupton, G. S. Ostrom, R. Quintana and J.-D. Woodroffe, *RSC Advances*, 2019, **9**, 22891-22899.
45. J.-C. Baret, *Lab on a Chip*, 2012, **12**, 422-433.
46. A. Fornell, F. Garofalo, J. Nilsson, H. Bruus and M. Tenje, *Microfluidics and Nanofluidics*, 2018, **22**, 75.
47. Acoustic Properties of Liquids, https://www.ondacorp.com/wp-content/uploads/2020/09/Liquids.pdf).
48. L. S. Roach, H. Song and R. F. Ismagilov, *Analytical Chemistry*, 2005, **77**, 785-796.
49. M. Pan, L. Rosenfeld, M. Kim, M. Xu, E. Lin, R. Derda and S. K. Y. Tang, *ACS Applied Materials & Interfaces*, 2014, **6**, 21446-21453.
50. C.-Y. Lee, C.-L. Chang, Y.-N. Wang and L.-M. Fu, *International Journal of Molecular Sciences*, 2011, **12**, 3263-3287.
51. H. Song, M. R. Bringer, J. D. Tice, C. J. Gerdts and R. F. Ismagilov, *Applied Physics Letters*, 2003, **83**, 4664-4666.
52. S. Li, M. Zeng, T. Gaule, M. J. McPherson and F. C. Meldrum, *Small*, 2017, **13**, 1702154.
53. X. Niu, S. Gulati, J. B. Edel and A. J. deMello, *Lab on a Chip*, 2008, **8**, 1837-1841.
54. N. Bremond, A. R. Thiam and J. Bibette, *Physical Review Letters*, 2008, **100**, 024501.
55. C. Huang, H. Zhang, S.-I. Han and A. Han, *Analytical Chemistry*, 2021, **93**, 8622-8630.
56. C. N. Baroud, M. Robert de Saint Vincent and J.-P. Delville, *Lab on a Chip*, 2007, **7**, 1029-1033.
57. M. Sesen, T. Alan and A. Neild, *Lab on a Chip*, 2014, **14**, 3325-3333.
58. A. R. Abate, T. Hung, P. Mary, J. J. Agresti and D. A. Weitz, *Proceedings of the National Academy of Sciences*, 2010, **107**, 19163-19166.
59. A. Fornell, Z. Liu and M. Tenje, *Microelectronic Engineering*, 2020, **226**, 111303.
60. S.-I. Han, H. Soo Kim and A. Han, *Biosensors and Bioelectronics*, 2017, **97**, 41-45.
61. D. R. Link, S. L. Anna, D. A. Weitz and H. A. Stone, *Physical Review Letters*, 2004, **92**, 054503.
62. J. H. Jung, G. Destgeer, B. Ha, J. Park and H. J. Sung, *Lab on a Chip*, 2016, **16**, 3235-3243.

63. Y. Wang, Y. Zhao and S. K. Cho, *Journal of Micromechanics and Microengineering*, 2007, **17**, 2148-2156.
64. M. R. Raveshi, S. N. Agnihotri, M. Sesen, R. Bhardwaj and A. Neild, *Sensors and Actuators B: Chemical*, 2019, **292**, 233-240.
65. D. Di Carlo, *Lab on a Chip*, 2009, **9**, 3038-3046.
66. A. L. Vig and A. Kristensen, *Applied Physics Letters*, 2008, **93**, 203507.
67. M. Hein, M. Moskopp and R. Seemann, *Lab on a Chip*, 2015, **15**, 2879-2886.
68. D. Lombardi and P. S. Dittrich, *Analytical and Bioanalytical Chemistry*, 2011, **399**, 347-352.
69. M. A. M. Gijs, *Microfluidics and Nanofluidics*, 2004, **1**, 22-40.
70. E. Brouzes, T. Kruse, R. Kimmerling and H. H. Strey, *Lab on a Chip*, 2015, **15**, 908-919.
71. Y. Jo, F. Shen, Y. K. Hahn, J.-H. Park and J.-K. Park, *Micromachines*, 2016, **7**, 56.
72. S.-Q. Gu, Y.-X. Zhang, Y. Zhu, W.-B. Du, B. Yao and Q. Fang, *Analytical Chemistry*, 2011, **83**, 7570-7576.
73. A. Lenshof, C. Magnusson and T. Laurell, *Lab on a Chip*, 2012, **12**, 1210-1223.
74. M. Wiklund, *Lab on a Chip*, 2012, **12**, 2018-2028.
75. K. Park, J. Park, J. H. Jung, G. Destgeer, H. Ahmed and H. J. Sung, *Biomicrofluidics*, 2017, **11**, 064112.
76. A. Fornell, K. Cushing, J. Nilsson and M. Tenje, *Applied Physics Letters*, 2018, **112**, 063701.
77. A. Fornell, M. Ohlin, F. Garofalo, J. Nilsson and M. Tenje, *Biomicrofluidics*, 2017, **11**, 031101.
78. I. Leibacher, J. Schoendube, J. Dual, R. Zengerle and P. Koltay, *Biomicrofluidics*, 2015, **9**, 024109.
79. O. Jakobsson, S. S. Oh, M. Antfolk, M. Eisenstein, T. Laurell and H. T. Soh, *Analytical Chemistry*, 2015, **87**, 8497-8502.
80. Acoustic Properties of Solids, https://www.ondacorp.com/wp-content/uploads/2020/09/Solids.pdf).
81. Acoustic Properties of Rubbers, https://www.ondacorp.com/wp-content/uploads/2020/09/Rubbers.pdf).
82. T. Franke, A. R. Abate, D. A. Weitz and A. Wixforth, *Lab on a Chip*, 2009, **9**, 2625-2627.
83. S. Li, X. Ding, Z. Mao, Y. Chen, N. Nama, F. Guo, P. Li, L. Wang, C. E. Cameron and T. J. Huang, *Lab on a Chip*, 2015, **15**, 331-338.
84. H. Bruus, *Lab on a Chip*, 2012, **12**, 1014-1021.
85. S. S. Sadhal, *Lab on a Chip*, 2012, **12**, 2600-2611.
86. J. J. Hawkes, R. W. Barber, D. R. Emerson and W. T. Coakley, *Lab on a Chip*, 2004, **4**, 446-452.
87. P. Augustsson and T. Laurell, *Lab on a Chip*, 2012, **12**, 1742-1752.

88. Z. Liu, A. Fornell, L. Barbe, K. Hjort and M. Tenje, *Biomicrofluidics*, 2019, **13**, 064123.
89. F. Petersson, L. Åberg, A.-M. Swärd-Nilsson and T. Laurell, *Analytical Chemistry*, 2007, **79**, 5117-5123.
90. M. C. Jo and R. Guldiken, *Sensors and Actuators A: Physical*, 2012, **187**, 22-28.
91. K. Cushing, E. Undvall, Y. Ceder, H. Lilja and T. Laurell, *Analytica Chimica Acta*, 2018, **1000**, 256-264.
92. P. Li, Z. Mao, Z. Peng, L. Zhou, Y. Chen, P.-H. Huang, C. I. Truica, J. J. Drabick, W. S. El-Deiry, M. Dao, S. Suresh and T. J. Huang, *Proceedings of the National Academy of Sciences*, 2015, **112**, 4970-4975.
93. L. Schmid, D. A. Weitz and T. Franke, *Lab on a Chip*, 2014, **14**, 3710-3718.
94. P. Li, Z. Ma, Y. Zhou, D. J. Collins, Z. Wang and Y. Ai, *Analytical Chemistry*, 2019, **91**, 9970-9977.
95. A. Fornell, P. Söderbäck, Z. Liu, M. De Albuquerque Moreira and M. Tenje, *Micromachines*, 2020, **11**, 113.
96. Y. Liao, J. Song, E. Li, Y. Luo, Y. Shen, D. Chen, Y. Cheng, Z. Xu, K. Sugioka and K. Midorikawa, *Lab on a Chip*, 2012, **12**, 746-749.
97. H. Klank, J. P. Kutter and O. Geschke, *Lab on a Chip*, 2002, **2**, 242-246.
98. H. Namgung, A. M. Kaba, H. Oh, H. Jeon, J. Yoon, H. Lee and D. Kim, *BioChip Journal*, 2022, DOI: 10.1007/s13206-022-00048-1.
99. A. A. Tseng, C. Kuan, C. D. Chen and K. J. Ma, *IEEE Transactions on Electronics Packaging Manufacturing*, 2003, **26**, 141-149.
100. C. Sun, N. Fang, D. M. Wu and X. Zhang, *Sensors and Actuators A: Physical*, 2005, **121**, 113-120.
101. R. Negishi, K. Takai, T. Tanaka, T. Matsunaga and T. Yoshino, *Analytical Chemistry*, 2018, **90**, 9734-9741.
102. R. Nielson, B. Kaehr and J. B. Shear, *Small*, 2009, **5**, 120-125.
103. A. Piruska, I. Nikcevic, S. H. Lee, C. Ahn, W. R. Heineman, P. A. Limbach and C. J. Seliskar, *Lab on a Chip*, 2005, **5**, 1348-1354.
104. F. Laermer and A. Urban, in *Ultra-thin Chip Technology and Applications*, ed. J. Burghartz, Springer New York, New York, NY, 2011, DOI: 10.1007/978-1-4419-7276-7_9, pp. 81-91.
105. Y. Feng, L. Huang, P. Zhao, F. Liang and W. Wang, *Analytical Chemistry*, 2019, **91**, 15204-15212.
106. M. Musterd, V. van Steijn, C. R. Kleijn and M. T. Kreutzer, *RSC Advances*, 2015, **5**, 16042-16049.
107. J. Schindelin, I. Arganda-Carreras, E. Frise, V. Kaynig, M. Longair, T. Pietzsch, S. Preibisch, C. Rueden, S. Saalfeld, B. Schmid, J.-Y. Tinevez, D. J. White, V. Hartenstein, K. Eliceiri, P. Tomancak and A. Cardona, *Nature Methods*, 2012, **9**, 676-682.

108. M. R. Lamprecht, D. M. Sabatini and A. E. Carpenter, *BioTechniques*, 2007, **42**, 71-75.

Acta Universitatis Upsaliensis

Digital Comprehensive Summaries of Uppsala Dissertations from the Faculty of Science and Technology 2143

Editor: The Dean of the Faculty of Science and Technology

A doctoral dissertation from the Faculty of Science and Technology, Uppsala University, is usually a summary of a number of papers. A few copies of the complete dissertation are kept at major Swedish research libraries, while the summary alone is distributed internationally through the series Digital Comprehensive Summaries of Uppsala Dissertations from the Faculty of Science and Technology. (Prior to January, 2005, the series was published under the title "Comprehensive Summaries of Uppsala Dissertations from the Faculty of Science and Technology".)

Distribution: publications.uu.se
urn:nbn:se:uu:diva-472081

ACTA
UNIVERSITATIS
UPSALIENSIS
UPPSALA
2022